

Trends in hydroclimate extremes: How changes in winter conditions affect seasonal water storage and baseflow and storage

Tejshree Tiwari¹, Hjalmar Laudon¹

¹Department of Forest Ecology and Management, Swedish University of Agricultural Sciences, SE-901 83 Umea, Sweden

Correspondence to: Tejshree Tiwari (Tejshree.Tiwari@slu.se)

Abstract. Northern ecosystems experience rapid climatic change at a rate where average temperatures are increasing above global averages. Yet, for the boreal undergoing accelerated climate warming, with average temperature increases exceeding the global mean. In snow-dominated catchments that, where cold-season conditions are reliant on the winter snow accumulation and spring melting for sustained stream flow essential for sustaining streamflow across preceding subsequent seasons, much remains unknown about how substantial uncertainty persists regarding the impacts of future warming on catchment water storage and baseflow are affected runoff dynamics. Here, we used utilized 40 years of hydrological data from the boreal Krycklan catchment, placed inset within a 130-year climate record from a nearby location station, to test evaluate how 27 extreme climate change indices have been affected can capture changes and how these trends in turn, can explain seasonal water storage and stream low flows flow during the winter and summer. Our results show that while annual temperatures have increased risen by 2.2 °C °C over the last past four decades, with even more distinct pronounced seasonal impacts were detected as exemplified by eight. Notably, six winter extreme indices demonstrating that winters have become warmer with less precipitation. The analysis also showed that summers have become warmer shown by four significant increases in climate indices. Using the significant winter indices to predict winter baseflow and winter two summer indices to predict summer baseflow were revealed distinct trends. We found that warm winters have led to increased winter stream runoff but reduced summer runoff. Predictive modelling indicated that the accumulated freezing degree day below zero days (AFDD<0) was were the best strongest predictor of winter minimum winter flow and, while a combination of AFDD<0 and Summer maximum summer temperature (MaxTmax) were the best predictor of summer explained variations in minimum summer flow. Additional isotopic Furthermore, analysis of stream flow streamflow partitioning found using water isotopes and the seasonal origin index (SOI) over the past 22 years revealed an increasing winter precipitation signal in winter runoff, accompanied by a declining contribution of winter rain/snow in stream runoff during winter over the last 22 years, as well as a decreased contribution to the preceding summer stream flow. These to summer streamflow. Together, these findings imply demonstrate that warmer warm winters have affected are fundamentally altering catchment-scale water storage and runoff patterns in the boreal catchment which can have flow partitioning, with important feedback on terrestrial ecosystems, particularly on water implications for water availability in later parts of and ecosystem functioning during the growing season in boreal landscapes.

Formatted: Font colour: Auto

Formatted: Left, Space Before: Auto, After: Auto

Formatted

1 Introduction

Over the past decades, high-latitude areas have undergone a warming trend exceeding the global average, with the region continuing to warm at a rate more than twice as fast as the rest of the world (Druckenmiller et al., 2021; Rantanen et al., 2022). The boreal zone is particularly sensitive to the changes in climate (Ali et al., 2024; Fu et al., 2023; (Seidl et al., 2020; Fu et al., 2023; Ali et al., 2024) as its thermal regime is strongly is affected by the snow cover. Hence, temperature changes are likely to affect snow accumulation and the timing of melt (Bouchard et al., 2024; Friesen et al., 2021; (Kim et al., 2012; Peng et al., 2013; Friesen et al., 2021, Bouchard et al., 2024), which are mechanisms important for regulating the length of the growing season and plant phenology (Easterling 2002, Cleland et al., 2007; Easterling, 2002; Way, 2011). Consequently, shifts in the timing of the onset and end of winter are among the most fundamental impactsanticipated effects of climate change in northern latitudes, which can increase the risk of severe, and in some cases irreversible ecological impacts. Yet, how changes in seasonal cycles, temperature and moisture regimes feedback on terrestrial ecosystems, biogeochemical cycles and hydrological eyelesbalance, remain largely unknown.

Winter conditions define the timing and magnitude of hydrological processes within northern catchments particularly as seen in river runoff (Barnett et al., 2005; Blöschl et al., 2017; Hryciuk et al., 2024; Murray et al., 2023; Hryciuk et al., 2024). For instance, temperatures below freezing are conducive for precipitation to accumulate as snow and ice, which is made available for groundwater recharge during melting. The freezing period is therefore determinesa key determinant of the amount of water stored in catchments based on temperature departure below zero, but also on the duration of the below-zero period and the subsequent melting rate (Nygren et al., 2020; (Simons, 1967; Stieglitz et al., 2001; Nygren et al., 2020). Any changes to the period of below freezing will ultimately affect the duration of the cold period with consequences for the water cycle leading to alterations in the flow regime (Blöschl et al., 2017). Already, current observed changes in the winter period indicateahave led to significant trendtrends in shorterice duration, laterfreezing period and earlierbreak-up dates based on long-term data from 1913–2014 in Sweden and Finland (Arheimer and Lindström, 2015; Hallerböck et al., 2022). Such results have consequential effects on soil freeze/thaw cycles, and lake and river ice dynamics (Kim et al., 2012; Peng et al., 2013) across the northern hemisphere. Despite aHowever, despite this growing body of literatureevidence about warm winters, the implications ofrapidly changing winters on groundwater recharge conditions,water storage and how this will affect proceeding seasonal runoff dynamics, are still elusive.

Changes in river runoff are essential factors for assessing the effectsimpact of climate change on the hydrological cycle as the discharge is highly dependent on precipitation (P), evapotranspiration (ET), and changes in water storage across the entire watershed area (White et al., 2007). One of the most prominent effects of changes in water flux can be seen during the low flow (baseflow) periods, which for a given catchment largely is regulated by the amount of water stored in the catchments. In high latitude and altitude regions with long winters, midwinter baseflow quantities are primarily reliant on the factors

Formatted: Font colour: Auto

Formatted

Formatted: Font: +Headings (Times New Roman)

Formatted: Space Before: 0 pt

Formatted

Formatted: Font: +Headings (Times New Roman)

Formatted

Formatted: Space Before: 0 pt

conducive to winter snowmelt or direct contributions from rain on snow. In contrast, summer low flows are often more dependent on water storage in soil and groundwater, often dominated by recharge from occurring during snowmelt. PreviousDespite the host of studies that have already shown demonstrated that snow melts earlier in years with less winter snow accumulation, resulting in earlier peak runoff in the spring (Hryciuk et al., 2024; Irannezhad et al., 2022; (Venäläinen et al., 2020; Irannezhad et al. 2022, Hryciuk et al. 2024). Understanding how such changes in winter conditions will affect preceding seasonal flow, resulting in decreasing summer baseflow trends (Murray et al. 2023), clear evidence on how winter climate affects runoff, and consequently catchment recharge is still lacking (Tiwari et al. 2018, 2019). Understanding how such changes in winter conditions will affect subsequent seasonal runoff patterns is largely reliant on identifying techniques that can detect changes in the duration, magnitude and intensity of the freezing period, and their application towards understanding how catchments' water recharge and storage is affected (Dierauer et al. 2018, Blahušáková et al., 2020; Dierauer et al., 2018).

A powerful technique for assessing changes in stream flow involves using the differences in the water isotopic signatures of $\delta^{18}\text{O}$ in precipitation across seasons (Allen et al. 2019). The seasonality of isotopic signals in precipitation presents the possibility of tracing the fraction of water arriving in winter that can either be stored in the catchment or become streamflow directly during the current or during succeeding seasons. Similarly, the SOI can be used to infer the fraction of winter precipitation that becomes stream runoff during the summer. Using isotopic signals to understand the water partitioning in catchments offers a possibility to trace the role of winter precipitation contributions to stream runoff that is not possible by using hydrometric measurements only. This can be done by adapting the seasonal origin index (SOI) to implicitly test the proportion of winter precipitation versus summer precipitation in stream water with $\delta^{18}\text{O}$ isotopes using the methods outlined in Allen et al. (2019). The results from the SOI analysis can then be used to test whether increases in winter runoff and decreases in summer baseflow are the results of changes in winter precipitation.

The techniques of identifying when changes in climate time series occur usually involve using models to detect the statistical departures from historical baselines (Alexander et al., 2006; Reeves et al., 2007; Wilming et al., 2020). However, monitoring trends in seasonal variables has become increasingly challenging, as traditional definitions of seasonality are insufficient to reflect changes associated with a fluctuating climate weather conditions. For instance, the most commonly used definitions (e.g. astronomical and meteorological) are static in both time and space (Trenberth 1983, Allen, and Sheridan, 2015; Trenberth, 1983). However, considerable, Considerable changes to transition periods (spring and fall) between the warmest seasons in the summer to the coldest season in the winter are often not adequately defined based on their spatiotemporal variability (Huschke, 1959; (Huschke 1959). As such, static definitions of seasons are insufficient to properly characterize seasonal timing and length that, which, are also likely to continue to change in the future. Currently, many indicators of seasonality changes are based on temperature-related impacts on ecosystems, and hence they provide estimates of changes in the seasonal timing of the growing season. Minimum, mean, and maximum daily temperature have been taken

Formatted: Font: +Headings (Times New Roman)

Formatted: Font: +Headings (Times New Roman)

Formatted: Font: +Headings (Times New Roman)

Formatted: Font: +Headings (Times New Roman)

Formatted: Font: +Headings (Times New Roman)

Formatted: Font: +Headings (Times New Roman)

Formatted: Font: +Headings (Times New Roman)

Formatted: Font: +Headings (Times New Roman)

Formatted: Font: +Headings (Times New Roman)

Formatted: Font: +Headings (Times New Roman)

Formatted: Font: +Headings (Times New Roman)

Formatted: Font: +Headings (Times New Roman)

Formatted: Font: +Headings (Times New Roman)

Formatted: Font: +Headings (Times New Roman)

Formatted: Font: +Headings (Times New Roman)

Formatted: Space Before: 0 pt

Formatted: Font: +Headings (Times New Roman)

Formatted: Font: +Headings (Times New Roman)

Formatted: Font: +Headings (Times New Roman)

Formatted: Font: +Headings (Times New Roman)

Formatted: Font: +Headings (Times New Roman)

Formatted: Font: +Headings (Times New Roman)

Formatted: Font: +Headings (Times New Roman)

Formatted: Font: +Headings (Times New Roman)

Formatted: Font: +Headings (Times New Roman)

Formatted: Font: +Headings (Times New Roman)

as the most important temperature characteristics in the analysis of climate change (Moberg et al. 2006, Cohen et al. 2014, Cassou and Cattiaux, 2016; ~~Cohen et al., 2014; Moberg et al., 2006~~). Various indices have been used in the literature to divide seasons, such as those based on temperature (Alexander et al., 2006; Hekmatzadeh et al., 2020) and phenology (Schwartz and Crawford 2001, Cleland et al., 2007; Peng et al., 2013; ~~Schwartz and Crawford, 2001~~) or moving average smoothing techniques to identify the time that temperature rises above or fall below long-term mean (Blöschl et al., 2017; Park et al., 2021) or defined thresholds such as the 75th and 25th percentile to identify the coldest and warmest periods (Zschenderlein et al., 2019). These studies suggest that the onset and offset of seasons depend on the geographical location of the study region and its specific purpose where a variable threshold should be used for determining the ~~season-onset/offset~~ start and end dates.

Another powerful technique for assessing changes in stream flow involves using the differences in the water isotopic signatures of $\delta^{18}\text{O}$ in precipitation across seasons (Allen et al., 2019). The strong seasonality in $\delta^{18}\text{O}$ isotopes with more depleted (lighter) isotopes in winter and enriched (heavier) in summer precipitation presents the possibility to trace the fraction of water arriving as snow in the winter that can either be potentially stored in the catchment or becomes streamflow in the current or proceeding seasons. Similarly, in the summer, the precipitation can be traced to contribute to either storage, streamflow or evapotranspiration (ET). Characterizing the partition of precipitation is therefore important for quantifying the amount of water available for recharging different hydrological storages for sustained stream flow in proceeding seasons.

In this study, we focus on understanding how long-term changes in temperature and precipitation affect baseflow runoff in a snowmelt-dominated boreal catchment during the winter and summer. To do this, we used a 40-year time series of climate data, placed in a 130-year context from a nearby station, to evaluate climate change-related trends. A shorter more detailed time series (30 years) was used to detect potential changes in extreme climate indices during the winter and summer. Winter and summer seasons were thermally defined (Contosta et al., 2020), which is in line with techniques used around the Baltic regions for assessing seasonal climate changes (Kejna and Pospieszynska, 2023; Ruosteenoja et al., 2015). We hypothesized that warmer winters with shorter duration periods below freezing (zero °C) would result in higher runoff during winter but exhaust the amount of water needed to sustain base flow in the proceeding summer. The isotope analysis of $\delta^{18}\text{O}$ in winter and summer precipitation was then used to corroborate the findings of the relative contributions of summer and winter precipitation to stream flow.

This study integrates long-term hydro-climatic trend analysis, seasonal extreme indices, and water isotope-based seasonal origin tracing to assess how changes in winter climate influence inferred water storage and seasonal runoff dynamics in a well-studied boreal catchment. Although the effects of snowmelt and warming on streamflow have been widely investigated, the direct role of winter climate in controlling water storage and baseflow remains poorly quantified. To address this gap, a combined approach was applied using historical trend analysis, indices of climate extremes, and stable isotope data to evaluate the effects of winter climate on seasonal streamflow. The first objective was to identify possible significant changes

Formatted: Font: +Headings (Times New Roman)

Formatted: Font: +Headings (Times New Roman)

Formatted: Font: +Headings (Times New Roman)

Formatted: Font: +Headings (Times New Roman)

Formatted: Font: +Headings (Times New Roman)

Formatted: Font: +Headings (Times New Roman)

Formatted: Font: +Headings (Times New Roman)

Formatted: Font: +Headings (Times New Roman)

Formatted: Font: +Headings (Times New Roman)

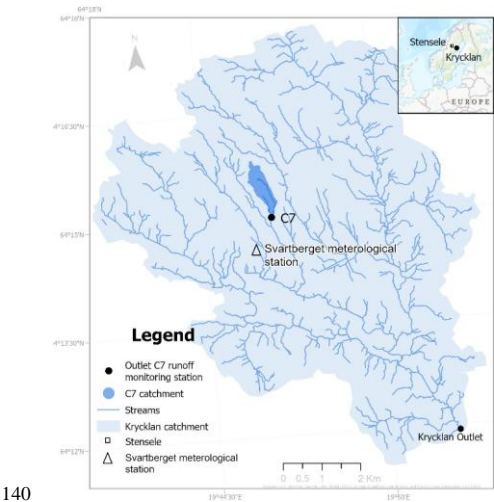
Formatted: Font: +Headings (Times New Roman)

Formatted: Font: +Headings (Times New Roman)

Formatted: Font: +Headings (Times New Roman)

130 in temperature trends using a 130-year historical dataset and assess their relationship to more recent changes captured in a
40-year on-site time series. Seasonal climate extremes were then derived from the last 30 years where we have high-
resolution data to identify extremes across the seasons. The second objective focused on quantifying the influence of these
climate extremes on key hydrological processes during winter and summer, using regression analysis to identify dominant
drivers of seasonal runoff. The final objective involved the application of the seasonal origin index (SOI), based on $\delta^{18}\text{O}$
135 isotope signatures, to quantify the relative contribution of winter precipitation to streamflow during winter and summer and
to verify consistency with observed hydroclimatic trends.

2 Methodology



140 **Figure 1** Map showing the Krycklan catchment, the location of the Svartberget meteorological tower in relation to the C7
catchment, the runoff monitoring station and the nearby Stensele meteorological station.

The Krycklan Catchment and Svartberget

145 This study focuses on the Krycklan catchment, which is a research infrastructure that has been monitored since the 1980s
[Laudon and Sponseller, 2018]. It is located in northern Sweden's boreal zone, approximately one hour from the city of Umeå.
Nested within the Krycklan catchment is the Svartberget catchment (C7), which has the longest monitoring high-quality record
in the region [Laudon and Sponseller 2018]. It is located in the boreal zone of northern Sweden, approximately one hour from

Formatted: Normal, Indent: Left: 0 cm, First line: 0 cm, Don't adjust space between Latin and Asian text, Don't adjust space between Asian text and numbers

Formatted: Font: +Headings (Times New Roman)
Formatted: Font: +Headings (Times New Roman), Font colour: Auto

the city of Umeå and the Baltic Sea. Nested within the Krycklan catchment is the Svartberget catchment (C7), which has the longest high-quality monitoring record of runoff in the region (Fig. 1) (Laudon et al., 2021). The 47 ha of C7 is dominated by forest (81%), primarily Norway spruce (*Picea abies*) and Scots pine (*Pinus sylvestris*) on till soils (81%) and peatland (19%). The location of Svartberget represents the conditions in Scandinavian boreal forests and is part of a network of stations within the Integrated Carbon Observation System (ICOS) - a European research infrastructure established to quantify and understand the greenhouse gas balance of the European continent and adjacent regions (Chi et al., 2020).

Meteorological measurements and data

Precipitation and temperature data from the Svartberget field station (Hygge, Fig. 1) was obtained from the SITES data portal (https://data.fieldsites.se/portal/). Precipitation (mm) was determined using daily (00-24) accumulated rain and snowfall amounts from manual measurement using a standard Swedish Meteorological and Hydrological Institute (SMHI) gauge with a windshield located 1.5 m above the ground (Climate monitoring program at SLU experimental forests and SITES Svartberget) (Laudon et al., 2013). The data available for Svartberget included two time periods (1982-2022) which consisted of daily mean precipitation and temperature used to detect long-term trends and (1992-2022) which consisted of average daily temperature, average daily minimum (min.) and average daily maximum (max.) temperature needed for the extreme climate change indices detection. Two data sets were used in this study because the earlier dataset 1982-1992 only provided one value for daily mean while 1992-2022 provided 10-minute recordings of temperatures from which daily minimum and maximums could be determined. Average daily minimum (Tmin) and maximums (Tmax) represent the coldest and warmest temperatures recorded in a day (Fig. S1), aggregated from 10-minute interval recording of temperatures. Included in this work Both Tmin and Tmax were used in the extreme indices to identify the coldest (minTmin) and warmest (maxTmax) in the season.

In addition to the Krycklan data, we have also used included a much longer-term dataset (1891–2004) from the SMHI meteorological station in Stensele, which is located approximately 150 km west of the Krycklan catchment (Fig. 1). The Stensele dataset is used to place the observed trends in from the past 40 years in the Krycklan catchment into a more longer-term climatic context. Temperature records from Stensele and Svartberget show strong agreement during their overlapping period (1982–2004), with an r^2 of 0.92 and a root mean square error (RMSE) of 0.05 based on daily average temperatures (Fig. S2). Minor systematic biases were identified: maximum temperatures were slightly higher in Svartberget, whereas minimum temperatures were slightly lower in Stensele. However, these differences were small (<3%) and did not affect the overall trends in the time series, which were the primary focus of this study. Therefore, the Stensele dataset was considered a reliable proxy for assessing historical climatic trends in the region.

Formatted: Font: +Headings (Times New Roman)

Formatted: Font: +Headings (Times New Roman)

Formatted: Font: +Headings (Times New Roman)

Formatted: Font: +Headings (Times New Roman)

Formatted: Font: +Headings (Times New Roman)

Formatted: Font: +Headings (Times New Roman)

Formatted: Font: +Headings (Times New Roman)

Formatted: Font: +Headings (Times New Roman)

Formatted: Font: +Headings (Times New Roman), Font colour: Auto

Formatted: Font colour: Auto

Formatted: Font colour: Auto

Formatted: Font colour: Auto

Formatted: Font colour: Auto

Formatted: Font colour: Auto

Formatted: Font colour: Auto

Formatted: Font colour: Auto

Formatted: Font colour: Auto

Formatted: Font colour: Auto

Formatted: Font colour: Auto

Formatted: Font colour: Auto

Formatted: Font colour: Auto

Formatted: Font colour: Auto

Formatted: Font colour: Auto

Formatted: Font colour: Auto

Formatted: Font colour: Auto

Formatted: Font colour: Auto

Formatted: Font colour: Auto

Formatted: Font colour: Auto

Formatted: Font colour: Auto

Formatted: Font colour: Auto

Formatted: Font colour: Auto

Formatted: Font colour: Auto

Formatted: Font colour: Auto

Runoff measurements and data

Runoff measurements from the Svartberget catchment (C7) were done using a field-based recording of hourly stage height and established rating curves to calculate the daily discharge from a weir located in a heated hut. The rating curve was established using the salt dilution technique and bucket-method measurements [Laudon et al., 2004]. Occasional missing data were gap-filled using the HBV model (Laudon et al. 2004). Occasional missing data (4%) were gap-filled using the HBV model (Karlsen et al. 2016, Karimi et al., 2022). The data available extended across 40 years from 1982-2022 which. The entire time series was used to show the long-term trends in minimum runoff (Qmin); however, the modelling was done using a subset of the data set (1992-2022) for the seasonal analysis to determinesynchronise with the low flow quantities extreme indices.

Seasonal definitions

Seasons were separated according to the thermal threshold definition using the frigid winter definition [Contosta et al., 2020], (Contosta et al. 2020), where winter was defined as the is a consistent frozen period when the air temperatures fell temperature is below 0°C for more than seven consecutive days (Fig. S3) without a longer period of greater than 0°C afterwards. We used the SMHI 10°C threshold for the definition of summer defined as, which is the period when the daily mean air temperature was greater than above 10°C for more than five consecutive days without a longer period of less than 10°C and. Summer ended when the daily mean air temperature was fell below 10°C for more than five consecutive days. Spring was defined as the season The spring period between winter and summer with was classified as the period when air temperature was above 0°C for more than seven consecutive days but less than 10°C for more than seven consecutive days. The autumn season was not used in this study; however, we checked the effects of autumn precipitation and runoff on mid-winter runoff and winter Qmin which did not show any significant effects (Fig. S4).

Extreme climate indices

We used 27 climate change indices that provide a consistent and traceable set of metrics that can be used to assess the long-term variability of extremes which was developed by the World Meteorological Organization (WMO) Expert team of Climate Change Detection and Indices [Donat et al., 2020]. These indices are designed to assess three aspects of temperature and precipitation regimes: i) intensity, ii) duration, and iii) frequency of events. These indices were then used to determine the variables within the winter, spring and summer (Table In total 27 climate change indices were used in this study, which were developed by the World Meteorological Organization (WMO) Expert Team of Climate Change Detection and Indices (Donat et al. 2020). These indices assess various aspects of temperature and precipitation variability including i) intensity, ii) duration, and iii) frequency of events. The indices identified were then determined for each seasonal block (winter, spring and summer (Table 1)) and used in the regression analysis to understand the relation to runoff. To address inhomogeneity in the dataset, we used the bootstrap technique to test if the trends in climate indices would vary depending on the window use i.e. 3 days, 5 days, 7 days) based on the description of the climate index (https://etccdi.pacificclimate.org/list_27_indices.shtml).

Formatted: Font colour: Auto

Formatted: Font colour: Auto

Formatted: Font colour: Auto

Formatted: Font colour: Auto

Formatted: Font colour: Auto

Formatted: Font colour: Auto

Formatted: Font colour: Auto

Formatted: Font colour: Auto

210 Temperature and precipitation extreme climate indices

To assess the temperature intensity, we extracted was assessed using seven variables from the daily time-series that describe average, minimum and maximum as follows: (i) the coldest daily maximum temperature (Min Tmax), (ii) the coldest daily minimum temperature (Min Tmin), (iii) the warmest daily maximum temperature (Max Tmax), (iv) the warmest daily minimum temperature (Max Tmin), (v) the mean difference between daily maximum and daily minimum temperature (diurnal temperature range), (vi) the number of days when Tmax < 0°C (icing days), and (vii) the accumulated degree days below 0°C (AFDD<0). The duration of ~~different thermal conditions in each season~~ extreme periods of the seasons was ~~described~~ categorized as (i) the number of days with at least six consecutive days when Tmin < 10th percentile (cold spell), and (ii) the number of episodes with at least six consecutive days with Tmax > 90th percentile (warm spell). The frequency of temperature events within each season was ~~determined using~~ identified as: (i) the percentage of days when Tmax < 10th percentile (cool days), (ii) the percentage of days when Tmin < 10th percentile (cool nights), (iii) the percentage of days when Tmax > 90th percentile (warm days), (iv) the percentage of days when Tmin > 90th percentile (warm nights), and (v) the number of days when Tmin < 0°C (frost days; Table S17-1).

The extreme intensity, duration, and frequency of seasonal precipitation patterns were ~~determined to also examined in terms of intensity, duration, and frequency. The precipitation~~ highlight extremes across the years. Precipitation intensity indices ~~included~~ was measured using: (i) maximum 1-day precipitation total, (ii) maximum 5-day precipitation total, (iii) sum of daily precipitation > 95th percentile (wet days), and (iv) sum of daily precipitation > 99th percentile (very wet days). ~~The while~~ duration of precipitation events were done using (i) the maximum number of consecutive wet days (precipitation > 1 mm) and (ii) the maximum number of consecutive dry days (precipitation). It should be noted that W and S are used in the regression models to distinguish between winter and summer variables.

230 Analysis: Trend detection and regression analysis

First, the Trends in extreme climate indices were assessed using the trend detection package in R (R Development Core Team [2021] was used Team, 2021), applied to detect trends and significant changes in the long-term dataset (1982–2022) datasets of average daily temperature, daily precipitation, and daily runoff (1982–2022). Then a. Analyses were conducted for both annual and seasonal analysis of the significant trends in the datasets (winter, spring, and summer seasons, was done using the) across 27 indices defined for each season, individually. Seasonal trends in baseflow (minimum Q) from winter and summer were also examined, examining trends in mean values and variability (standard deviation). The coefficient of regression (r^2) was used to identify the direction of the trends and the p-value Mann-Kendall test was used to determine the trend direction and p-values for significance of the changes. To determine/identify which of the significant extreme-climate indices could explain the baseflow during winter and summer, we used a best explained minimum seasonal runoff (Qmin), stepwise linear regression analysis in was performed using Minitab® Statistical Software 2021 to predict how the previous seasons' significant indices

affected seasonal baseflow runoff (2021). For winter, we used the Q_{min} , significant variables for winter temperature and precipitation of the winter season. For indices were used, while summer we used the preceding seasons which included Q_{min} was predicted based on significant variables/indices from winter, spring, and summer to predict summer baseflow runoff.

$\delta^{18}O$ and Seasonal Origin index

As a verification test for understanding the contributions of seasonal precipitation to annual runoff, the analysis of $\delta^{18}O$ isotopes was done/carrried out. Samples were collected at regular intervals from 2002 to 2022 in precipitation (n=1930) and stream water (n=821). Precipitation sampling was done manually using national standard precipitation gauges with a windshield where samples were collected in dark glass bottles with a hermetic lid to minimize evaporation during storage. These rain gauges were heated during winter to avoid snow accumulation in the collection funnels and enable sampling during the frozen period. Stream water samples were collected weekly with more frequent sampling during the snowmelt season in similar bottles as precipitation samples. During the winter, a heated weir house enables sampling throughout the frozen season. Both precipitation and stream samples were analyzed/analysed using a Picarro cavity ringdown laser spectrometer (L1102-i and L2130-i after September 2013) and the vaporizer module (V1102-i and later the A0211) (See Peralta-Tapia et al. [2016] for more details). Peralta-Tapia et al. (2016) for more details). Calibration of the isotopic signatures of water was done using internal laboratory standards calibrated against three International Atomic Energy Agency (IAEA) official standards, the Vienna Standard Mean Ocean Water (VSMOW), the Greenland Ice Sheet Precipitation (GISP) and the Standard Light Antarctic Precipitation (SLAP) [Coplen, 1995] (Coplen 1995).

The $\delta^{18}O$ data was then used in the seasonal origin index analysis to test whether winter or summer precipitation is overrepresented in annual streamflow [Allen et al., 2019]. The SOI show The $\delta^{18}O$ data was then used in the seasonal origin index (SOI) analysis to test whether winter or summer precipitation is overrepresented in seasonal streamflow (Allen et al. 2019). The SOI is a technique that can be used to identify the prevalence of winter versus summer precipitation sources in stream water due to the inherent differences in the winter and summer precipitation signals. This can be done using the deviation of annual average discharge from annual precipitation and scales the deviation by the strength of the seasonal signals using eq.1

$$SOI_{\bar{Q}} = \frac{\delta_{\bar{Q}} - \delta_{\bar{P}}}{\delta_{\bar{P}} - \delta_{\bar{P}_W}} \text{ if } \delta_{\bar{Q}} > \delta_{\bar{P}} \quad \text{eq.1}$$

$$\frac{\delta_{\bar{Q}} - \delta_{\bar{P}}}{\delta_{\bar{P}} - \delta_{\bar{P}_W}} \text{ if } \delta_{\bar{Q}} < \delta_{\bar{P}}$$

Where $\delta_{\bar{P}_S}$, $\delta_{\bar{P}_W}$, $\delta_{\bar{P}}$ and $\delta_{\bar{Q}}$ represents the $\delta^{18}O$ values of summer, winter, and volume-weighted annual precipitation in the C7 catchment and annual volume-weighted mean streamflow $\delta^{18}O$ respectively. To determine the SOI of winter and summer, we calculate the SOI of individual streamflow samples $\delta_{\bar{Q}}$ using their individual isotope ratios. The January samples were used to represent the winter, and the July samples were used to represent the summer isotopic signals. Linear regression was then used

Formatted: Font: Times New Roman

Formatted: Superscript

Formatted: Superscript

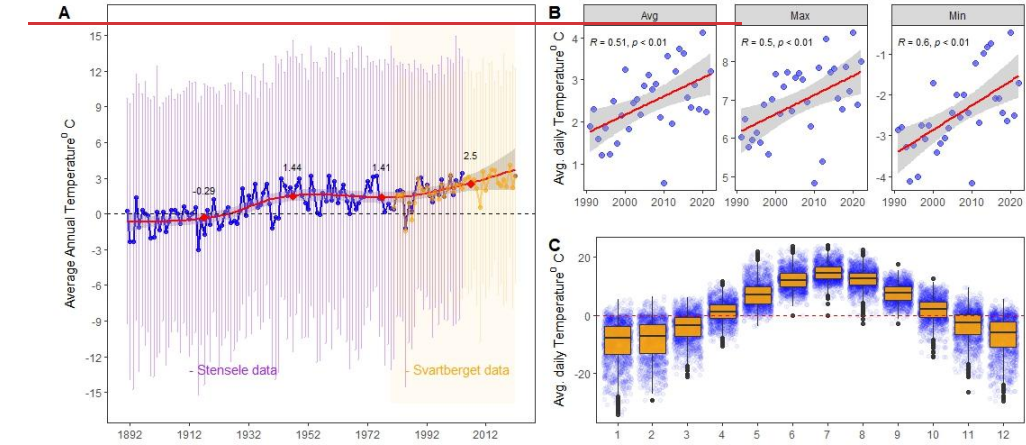
to show the trend in SOI across time for proportion of winter precipitation in winter and summer baseflow where positive SOI_Q (closer to 1) in the summer indicates a larger fraction of summer precipitation in streamflow. Similarly, increasing negative SOI_Q (closer to -1) during the winter means greater contributions from winter precipitation to stream flow.

Results

Trends in temperature, precipitation and runoff in Svartberget

Over the last four decades, the increase in temperature has accelerated by 2.2 °C where the long-term average daily temperature trend changed from 0.5°C/100 years in 1980 to 3.42 °C in 2022 across the Svartberget dataset (Fig. 1-A2A).

Placing these trends into a much longer perspective by using a time series that extended to 1892 from the nearby SMHI-Stensele meteorological station, we note that the increasing trends observed in the Svartberget is a part of the much longer-term temperature trend that extends over a 100 years. Looking back at the 30-year normal period trends over this time period, we can observe that at the beginning of the century, 1892-1922 annual average air temperature was much colder (-0.529 °C) than the most recent periods 30-year normal period (1993-2022) which was warmer (2.5 °C) (Fig. 1-A2A).



285

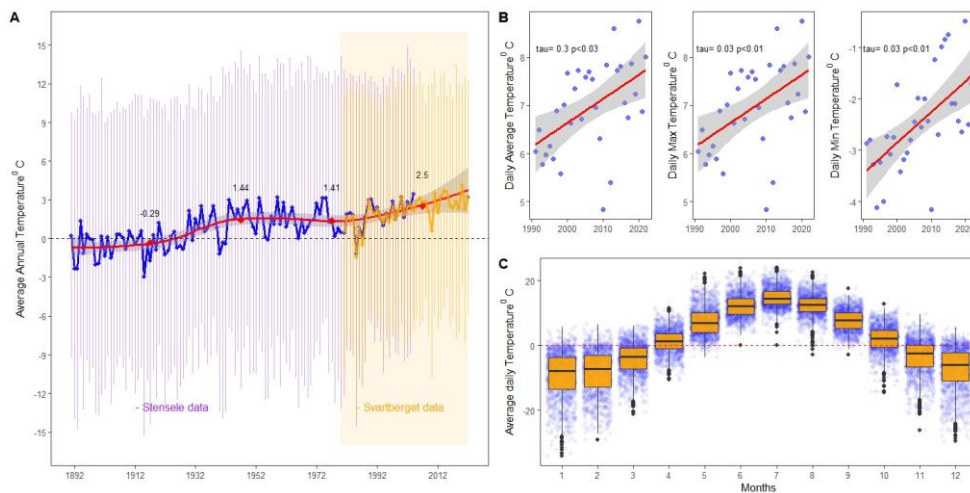


Figure 12 Trend in long-term climate temperature in the Krycklan catchment annually in showing; (A) the relation to the much longer-term trend-based on time series from the SMHI-Stensele data (1891-2004) (A); (B) trends in average daily air temperature (Avg.), maximum (Max.) daily air temperature and (C) minimum (Min.) daily temperatures, and variability in daily temperatures in the months across the year (B), trends in average annual air temperature, maximum (Max) annual air temperature and minimum (Min) daily temperatures (C), across 30 years from 1992-2022. Purple In panel A, the red symbols indicate the average within a 30-year period from 2022 backwards while purple and orange error bars in panel A represent the standard deviation in the dataset, and Stensele and Svartberget datasets, respectively. The grey shaded area in panel B represents the standard error in the datasets and the blue jitter dots in panel B represent daily average temperatures in Svartberget. Red dots indicate the average within a 30-year period from 2022 backwards in panel A.

A closer look at the last 30 years of variability in temperatures in the Krycklan catchment (1992-2022) showed annual average temperatures ranging from 0.5 to 5 °C across the years increasing from 1.95 °C in 1992 to 3.21 °C by 2022 (Fig. 1B). The annual-average minimum temperature ranged from -4.1 to -0.4 °C with, 2B) when observing the coldest long-term trend line. Trends in average monthly daily temperatures occurring in January ranging from -18.7 to -6 °C (Fig. 1C). There is a showed significant increase in minimum temperatures from 1992 to 2022—observed annual averages (0.34 °C to 1.6 °C indicating an increase of 1.8 °C, $p < 0.03$), average daily maximums (0.3, $p < 0.01$) and average daily minimums (0.3, $p < 0.01$) during the coldest month (Fig. 1B). These changes in minimum temperatures suggest that the winter seasons on average are becoming warmer period 1992-2022 (Fig. 2B, Table S1). Annual average maximum temperatures ranged from 4.8 to 8.7 °C with an increasing trend from 6.4 °C in 1991 to 7.8 °C in 2022 also showing indicating an increase in maximum temperature of 1.4 °C across the 30 years. Warmest periods occur during month 7 (July) when the temperature ranges from 17.4 ° to 25.2 °C (Fig. 1C). Trends in average daily temperatures showed significant increases in observed annual averages ($r^2 = 0.26$, $p < 0.05$), average daily minimums ($r^2 = 0.36$, $p < 0.05$) and average daily maximums ($r^2 = 0.26$, $p < 0.05$) during the period 1992-2022 (Fig.

Formatted: Font: 8 pt

Formatted: Not Superscript/ Subscript

Formatted: Font colour: Auto

S4)-2C). The annual average minimum temperature ranges from -4.1 to -0.4 °C with the coldest average monthly temperatures occurring in either January or February, ranging from -20.6 to -7.6 °C (Fig. 2C). There is a significant increase in minimum temperatures from 1992 to 2022 (-3.4 °C to -1.6 °C) indicating an increase of 1.8 °C during the coldest months (Fig. 2B). These changes in minimum temperatures suggest that the winter seasons on average are becoming warmer.

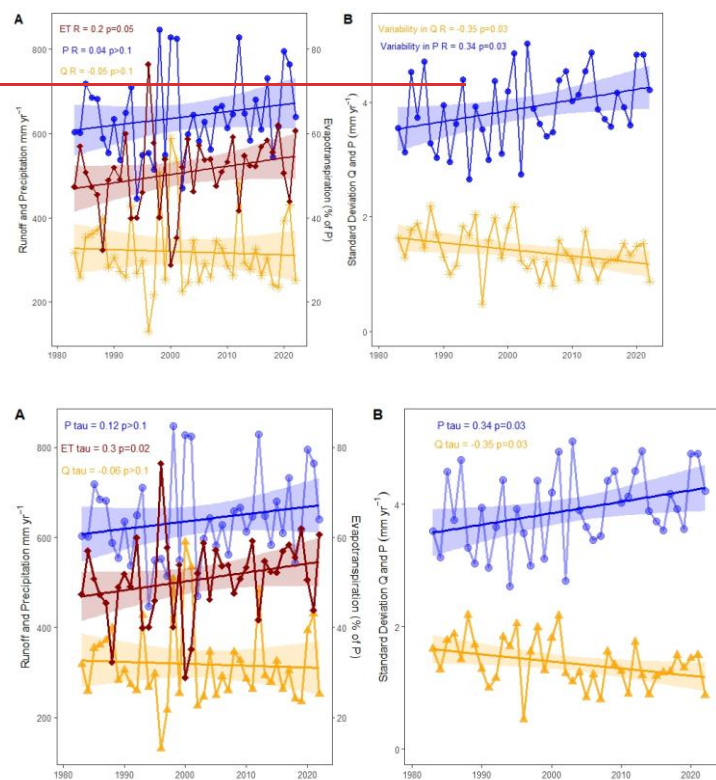


Figure 2 Variability and long-term trends in total annual precipitation (P) and total annual runoff (Q) from the Krycklan catchment across 40 years showing the differences in the percentage of precipitation (P) from runoff (Q) that represents evapotranspiration (ET) (panel A). The variability as measured by the standard deviation in runoff (Q) and precipitation (P) during the time period is shown (in panel B). The shaded areas represent the standard error in the datasets.

The long-term trends 1982-2022 showed an increase in daily total annual precipitation from 1982-2022 showed a decreasing trend while total annual runoff increased showed a decrease when fitted with a linear regression (Fig. 2A3A). A closer look at

Formatted: Font colour: Auto

Formatted: Font colour: Auto

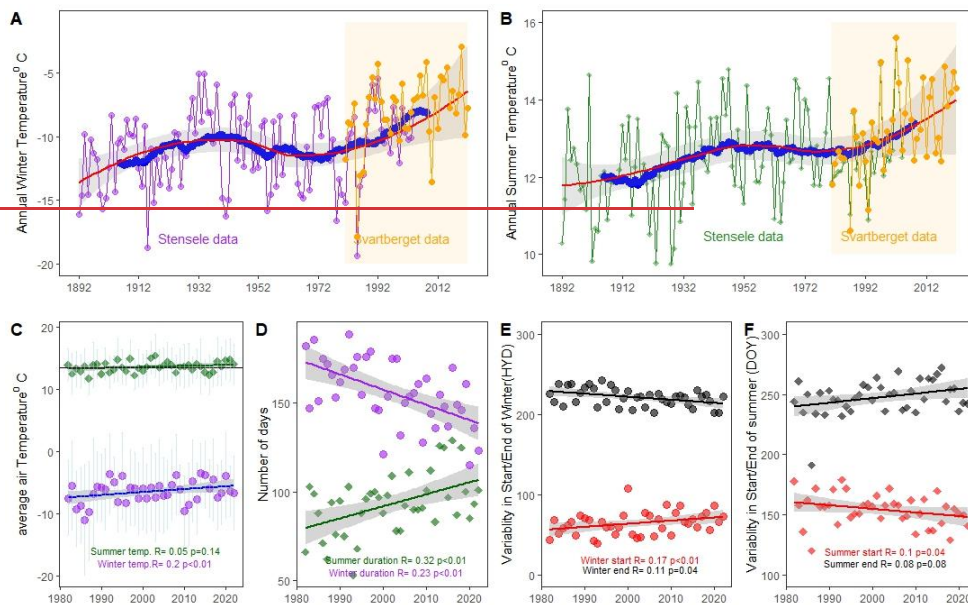
the variability in both the total annual precipitation and runoff across the time series indicated that trends ~~in the daily values~~ were variable across the years decreasing in the period 1982-1997 followed by an increase towards 2022 (~~Fig. S2 as shown with the loess regression (Fig. S5, Table S1). It should be noted that this variability as measured by the standard deviation in runoff has decreased by 0.5 mm day⁻¹ from 1.6 mm day⁻¹ to 1.1 mm day⁻¹ while the variability in precipitation increased significantly from 3.5 to 4.2 mm day⁻¹ during the same period (Fig. 3B).~~ Annually, on average the highest total monthly precipitation occurred in July (86 mm on average across the years) while the lowest occurred in April (28 mm). The annual average precipitation was 650 mm per year with the lowest records occurring in 1994 and 2002 (446 and 470 mm respectively) (Fig. 2A3A) when July/August precipitation was less than 30% of the long-term July/Aug values. The average total annual runoff was 318 mm year⁻¹ with the lowest runoff occurring in February (5.8 mm month⁻¹) and the highest in May (spring flood) with 96 mm month⁻¹ accounting for 30% of the total annual runoff. While no significant trends in total annual precipitation and runoff could be detected: (tau = 0.12 p > 0.1, tau = -0.06, p > 0.1, for P and Q respectively), ET during the same period calculated from the differences between precipitation and runoff showed a generally increasing annual trend (Fig. 2). ~~It should be noted that the variability in runoff has decreased by 0.5 mm day⁻¹ from 1.6 mm day⁻¹ to 1.1 mm day⁻¹ between the periods of 1982-2022 (Fig. 2B, Table S2, Fig. S20.3, p = 0.02) (Fig. 3A).~~

Formatted: Font colour: Auto, Border: : (No border)

Variability in winter and summer climate variables

The significant changes in minimum and maximum annual temperatures prompted further investigations into the variability of temperature and precipitation during the coldest (winter) and warmest (summer) seasons. ~~To do this, we isolated the freezing period by classifying winter as the period when the average air temperature consistently is below zero, and the summer season as when the average air temperature increases above 10°C consistently for summers (Fig. S3).~~ The temperature trends in Svartberget during the winter and summer are consistent with the longer-term time series from the SMHI-Stensele dataset (Fig. 3A4A and B). The analysis showed significant increases in average winter temperatures (tau = 0.12, p = 0.14) where daily averages ranged from -30.7 °C to 6.1 °C with the coldest winters occurring in 1986 and 2010 (with average winter temperatures of -11 and - 9.5 °C) while the warmest winters in 2014 and 1992 (-average winter temperatures -3.7 °C and 3.2 °C) (Fig. 3C4C). The duration of the winter period changed from 171 days to 140 days over the 30 years showing a loss of 31 days with the start of winter shifting 16 days later and ending 15 days earlier (Fig. 3D4D and E). Summers on the other hand, while showed warmer average temperature trends (r² = 0.0512, p = 0.14), the analysis indicated that the season was getting longer (22 days) moving from 80 days in early 1982 to 102 days in 2022 (Fig. 3D4D and F). The start and end of summers were shifting on average ~~twelve~~eleven days earlier and later respectively (Fig. 3F4F). Total precipitation during winter has decreased but increased during the summer, however, neither of these trends was significant. ~~p < 0.05 (Fig. S4 (Table. 1).~~

Formatted: Strikethrough



Formatted: Keep with next

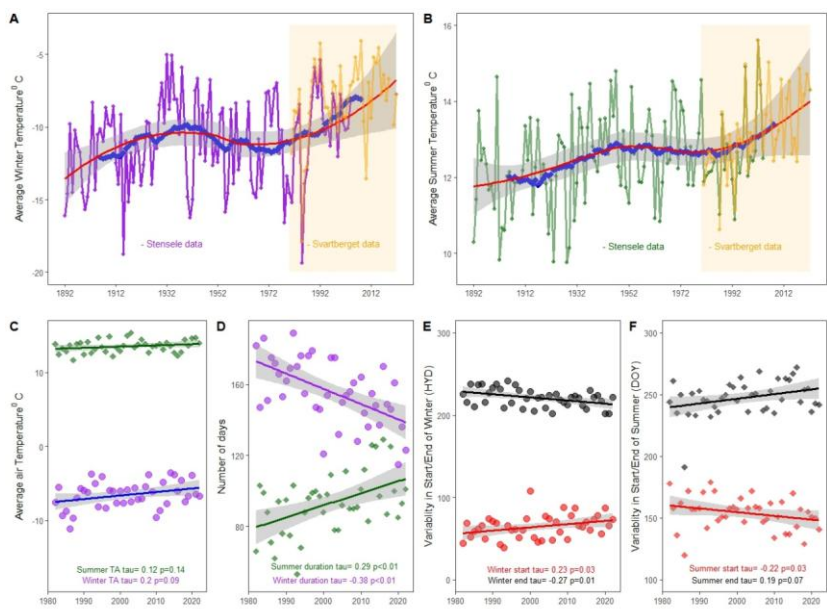


Figure 34 Variability in seasonal temperature across 40 years in the Svarterget-Krycklan catchment (blueorange box) showing changes in temperature during the winter (A) and Summer (B) in relation to the SMHI Stensele longer-term dataset (1891-2004). The variability in annual air temperature (C) and duration are shown in panels C and (D) is represented by purple symbols for the winter (purple) period and green symbols for the summer (green) period. Changes in the start (red) and end (black) of the winter (circle) and summer (diamonds) are depicted in panels E and F, respectively. Standard errors in the datasets (A, B, D, E, F) are shown as grey shading.

Formatted: Font: 8 pt

Formatted: Font: Not Bold

Table 1 Extreme climate indices used in the analysis of 30 years of climate data from 1992-2022 showing the description of the indices and the results of the Mann Kendall trend test (tau) and significant (p values). A detailed description of each index can be found at the World Meteorological Organization Expert Team of Climate Change Detection and Indices (http://etccdi.pacificclimate.org/list_27_indices.shtml; commissioned by the World Meteorological Organization Commission for Climatology ((CCI)/CLIVAR/ JCOMM).

Extreme Climate Indices		Definition	Unit	Trend - Mann Kendall test (tau)		
				Winter	Spring	Summer
2.7 Extreme Climate change indices	Intensity	-	-	-	-	-
	Min Tmax	Coldest avg. daily max. temp.	o C	0.02, p =0.8	-0.02, p =0.87	-0.09, p =0.45
	Min Tmin	Coldest avg. daily min. temp.	o C	0.11, p =0.3	0.02, p =0.86	-0.03, p =0.82
	Max Tmax	Warmest avg. daily max. temp.	o C	0.05, p =0.6	-0.03, p =0.79	0.33, p <0.01
	Max Tmin	Warmest avg. daily min. temp.	o C	-0.05, p =0.6	0.04, p =0.73	0.11, p =0.36
	Diurnal temperature range	Mean difference between daily max. and daily min. temp.	o C	0.29, p =0.01	-0.04, p =0.72	0.04, p =0.70
	AFDD <0	Accumulated freeze degrees on days where avg. daily air temp. was less than 0°C	o C	-0.42, p <0.01	0.04, p =0.71	
	Freeze thaw days (Tmax >0 Tmin <0)	The No. of days when the avg. daily max. air temp. was more than 0°C and the avg. daily min. air temp. was less than 0°C	Days		-0.04, p =0.70	
	Duration					
	Growing season length	No. of days between the first occurrence of six consecutive days with Tmean >5°C and first occurrence of consecutive 6 days with Tmean <5°C	Days			0.2, p =0.01
	Cold spell duration indicator	No. of days with at least six consecutive days when Tmin < 10th percentile	Days	-0.26, p =0.03	0.05, p =0.70	-0.006, p =0.97
	Warm spell duration indicator	No. of days with at least six consecutive days when Tmax > 90th percentile	Days	-0.09, p =0.4	-0.06, p =0.63	-0.03, p =0.82
	Frequency					
	Cool days	Share of days when Tmax < 10th percentile	%Days	-0.01, p =0.94	-0.06, p =0.60	0.17, p =0.17
	Cool nights	Share of days when Tmin < 10th percentile	%Days	-0.24, p =0.04	-0.07, p =0.64	0.28, p =0.02
	Warm days	Share of days when Tmax > 90th percentile	%Days	-0.01, p =0.94	-0.08, p =0.60	0.21, p =0.09
	Warm nights	Share of days when Tmin > 90th percentile	%Days	0.09, p =0.48	-0.08, p =0.50	0.22, p =0.07
	Frost days	No. of days when Tmin < 0	Days	-0.29, p =0.01	-0.10, p =0.43	-0.08, p =0.56
	Icing days	No. of days when Tmax < 0	Days	-0.23, p =0.07	-0.10, p =0.42	
	Precipitation					
	Intensity					
	Max 1-day precip.	max. 1-day precip. total	mm	-0.08, p =0.54	-0.11, p =0.42	0.09, p =0.44
	Max 5-day precip.	max. 5-day precip. total	mm	0.05, p =0.67	-0.13, p =0.32	
	Simple daily intensity index	Total precip. divided by the No. of wet days (i.e., when precip. > 1.0 mm)	mm	0.02, p =0.83	0.15, p =0.27	0.17, p =0.16
	Contribution from very wet days	Sum of daily precip. > 99th percentile	mm	0.05, p =0.66	0.15, p =0.27	0.05, p =0.68
	Contribution from wet days	Total precip. from days >1 mm	mm	-0.13, p =0.33	-0.17, p =0.16	0.12, p =0.34
	Duration					
	Consecutive wet days	max. No. of consecutive wet days (i.e., when precip. >1 mm)	Days	0.04, p =0.75	-0.21, p =0.17	
	Consecutive dry days	max. No. of consecutive dry days (i.e., when precip.	Days	-0.20, p =0.11	-0.21, p =0.17	0.14, p =0.28
	Frequency					
	Heavy precip. days	No. of days when precip. >10 mm	Days			0.10, p =0.46
	Very heavy precip. days	No. of days when precipitator >20 mm	Days	0.10, p =0.42		
	Total snow days	No. of day when TA> 0	Days	-0.38, p =0.002		
	Runoff					
	Winter Qmin (1981–2022)	Min. winter runoff	mm day ⁻¹	0.31, p =0.004		
	Summer Qmin (1981–2022)	Min. summer runoff	mm day ⁻¹			-0.03 p>0.1

370

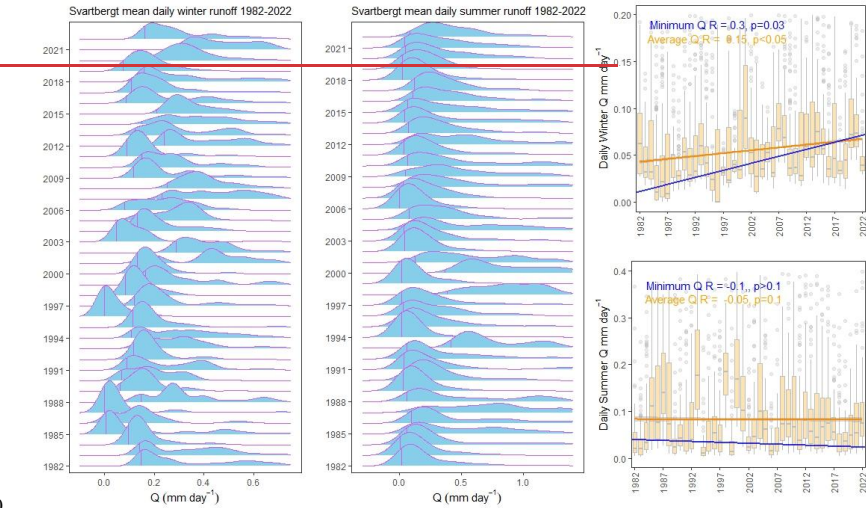
Extreme climate indices

Trends in extreme indices during the winter suggest that winters are becoming warmer with significant increases in minimum temperatures (Tmin, MinTmin, Diurnal diurnal temperature range, AFDD <0, Cold cold spell duration indicator, Cool, cool nights, and Frost frost days) and total snow days (Table S41). The extreme climate change indices during spring showed no significant trends ($p > 0.05$) across the 30-year period. Analysis of summer seasons showed significant increases ($p < 0.05$) in the Max-Tmax MaxTmax (warmest average daily maximum temperatures) ($p < 0.05$) and growing season length, warm days, and warm nights (Table S41, Fig. S5-S6). No significant increase in precipitation indices was found during summer.

375

Formatted: Font colour: Auto

Variability in seasonal runoff data



380

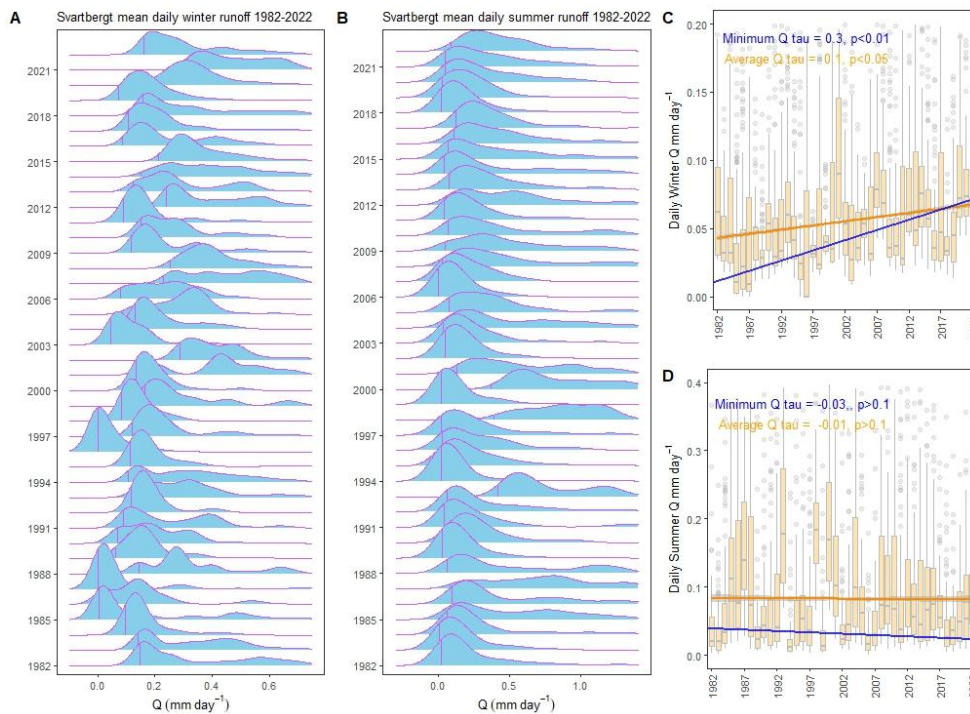


Figure 45 Variability and trends in seasonal runoff from showing hydrograph during the winter (A) and Summer (B) in the C7 catchment across. The minimum flow in each year during the winter and summer seasons showing are identified as vertical lines each year. The annual variability of winter runoff is shown as boxplots (C) and trends in minimum (blue line) and average (orange) across the time period and trends in daily runoff across the seasons-years. In panel D, the boxplots show the annual variability of summer runoff (D) and trends in minimum (blue line) and average (orange) runoff across the years.

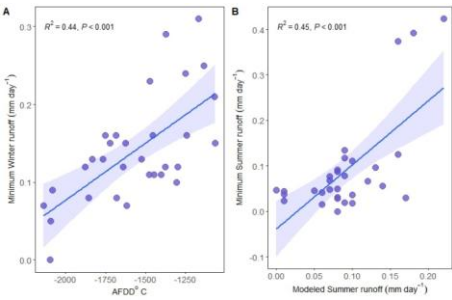
Looking at the runoff time series between 1982-2022, we observed similar increases in winter trends in Q_{\min} ($\tau = 0.3$, $p < 0.01$). Winter runoff over the last 40 years showed an increasing trend in minimum runoff ($r^2 = 0.3$, $p = 0.03$) suggesting higher winter baseflows from 1982 to 2022. Runoff during the winter Q_{\min} varied between 0.001-0.05 mm day^{-1} per day with total season runoff during the winter varying between 18 mm day^{-1} and 144 mm day^{-1} . On average runoff ranged between 0.1 mm day^{-1} and 1.1 mm day^{-1} per day with the lowest runoff was recorded in 1996, and the highest runoff occurring was recorded in 2007 (Fig. 45C). During the summer, the minimum trends in runoff were also decreasing ($r^2 = \tau = -0.0501$, $p = 0.14$) with average daily runoff varying from 0.13 mm day^{-1} to 2.45 mm day^{-1} . Daily minimums varied from 0.01 mm day^{-1} to 0.424 mm day^{-1} while maximum runoff during the summers varied from 0.8 mm day^{-1} to 21.9 mm day^{-1} . The

Formatted: Left

395 driest years were recorded in 2006 (where the average daily minimum was 0.03 mm day⁻¹) and the wettest years were recorded
 400 in 1986 (1993 where the average daily minimum was 0.4642 mm day⁻¹) (Fig. 4)-5D).

Model of changes in runoff

To understand which hydroclimatic variable was driving the minimum runoff during seasonal low-flow periods the winter and
 400 summer seasons, we use a stepwise linear regression analysis to identify the best explanatory climate variables of the
 preceding/succeeding season for runoff in Minitab Statistical Software 17. A trend detection test was first performed in R to
 determine if there was a significant trend in each seasonal data set- using the trend package and Mann Kendal trend test. Only
 the extreme climate variables that showed a significant trend (p <0.05) were used in the seasonal runoff regression models.



405 **Figure 6.** The best explanatory climate indices of winter minimum runoff (Qmin) were the accumulated freeze degree days below
 zero (AFDD<0) (W_Qmin=1.26 - 0.0065 AFDD <0) for the winter and the summer (S_Qmin= 0.3 - 0.007 S_Max Tmax + 0.00004
 W_AFDD <0). The standard error in each dataset is represented by the blue shades.

From this analysis, we found that the winter accumulated degree days below zero (AFDD<0) were the best explanatory variable
 of minimum-runoff-Qmin during the winter (r²=0.44 p<0.05)-, W_Qmin=1.26 - 0.0065 AFDD <0) (Table S1). The analysis
 showed that winters with fewer AFDD<0 (warmer winters e.g. 2014 when AFDD was 1053 °C), were associated with higher
 410 winter baseflow-Qmin (0.2 mm day⁻¹) while winters with more AFDD<0 (cold winters e.g. 1994 when AFDD was -
 2138 °C) showed low winter baseflow-Qmin (0.1 mm day⁻¹) (Fig. 5)-6A). The best explanatory factor of runoff variability in
 summer baseflow-Qmin was a multivariate model (S_Qmin= 0.3 - 0.007 MaxTmax + 0.00004 W_AFDD <0) which included
 winter variables W_AFDD<0 and Summer MaxTmax (r²=0.45 p<0.05) as found from the stepwise linear regression model.
 The three years (1993, 1998 and 2000) were the largest outliers in the model because these were the wettest years when
 415 minimum runoff was above 0.35 mm day⁻¹ (Fig. 6B)-5B).

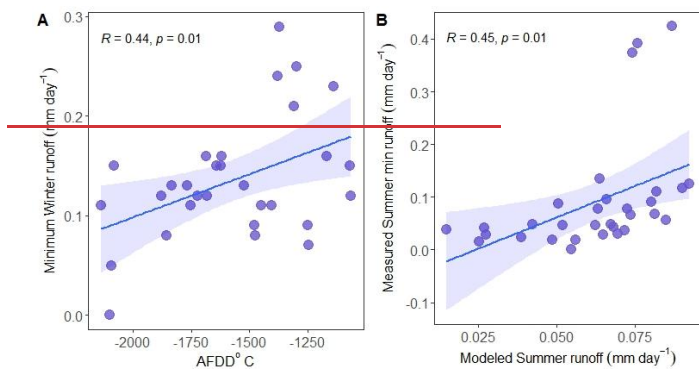


Figure 5 The best-explanatory climate indices of winter baseflow were the accumulated freeze degree days below zero (AFDD<0) ($Q_w = 1.26 - 0.0065 \text{ AFDD} < 0$) for the winter and the summer ($Q_s = 0.3 - 0.007 \text{ Summer Max Tmax} + 0.00004 \text{ Summer AFDD} < 0$)

Isotope analysis using season origin index (SOI)

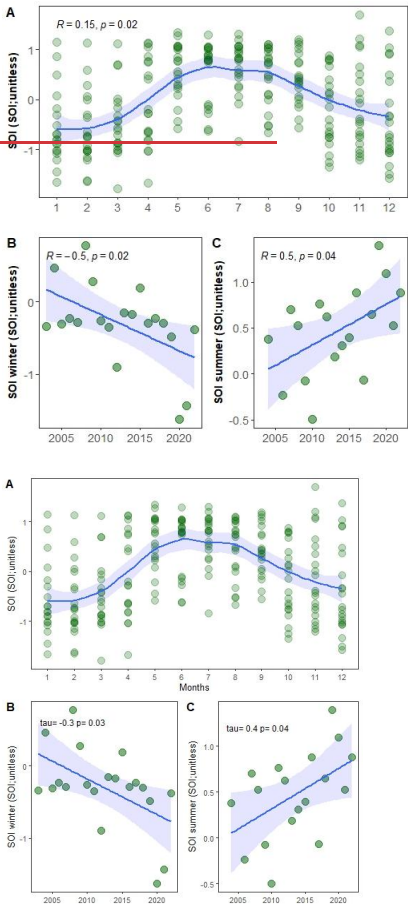


Figure 67 Variability in season origin index (SOI) daily values from 2003-2022 in the C7 catchment with a loess curve (blue) representing average monthly SOI values (A). The fraction of midwinter precipitation and midsummer precipitation that becomes stream flow each year is shown in panels B and C fitted with linear regression.

InvestigatingTo test if the changes in runoff identified during the winter and summer seasonal analysis of Qmin could be explained by the contribution of seasonal precipitation to stream flow, we use the SOI analysis to further understand observed

trends. This analysis showed that the SOI in the C7 catchment showed strong seasonality across the yearyears when looking at monthly variability. In the colder months, SOI averaged -0.5 in December, January and February while in the warmer months, averages increased to 0.5 in June, July, and August. (Fig. 7A). A closer look at the winter SOI in January showed that a greater fraction of the winter precipitation was represented in annualthe stream flow across time as indicated by the SOI values shifting closer to -1 (typical of mid-winter precipitation) (Fig. 7B). This corresponded with the higher Qmin during the winter identified using the runoff analysis.6B). The SOI in the summer (July) increased-with a shift closer to 1 (typical of midsummer precipitation) indicating that a larger fraction of summer precipitation in later years became stream flow relative to the total annual-precipitation suggesting a shift away from the mid-winter signal (-1) (Fig. 6C).7C). This infers a lower contribution of winter precipitation to summer stream flow corresponding to the decreasing trends in Q min during the summer identified using the Qmin trend analysis.

Discussion

Analysis of extreme climate indices over the past 40 years in the boreal Krycklan catchment has shown that the most pronounced changes occurred in the winter where warmer winters with less precipitation as snow have increased baseflowminimum runoff quantities during the winter, which resulted in an exhaustion of water left for baseflow in the proceedingssucceeding summers. The changes in runoff during the winter and summer are alsofurther supported by isotope analysis that shows an increasing contribution of winter precipitation to winter runoff and a decreasing contribution to summer runoff. Although theThese results are based on thea 40-year time series, these changes observed are part ofare consistent with a longer-term trend dating back to 1891 from a nearby meteorological station (Stensele), which has acceleratedshows an acceleration, particularly in the last decades (Fig 1A, 3A2A, 4A, and B). Nevertheless, the 40-year time series of both meteorological and hydrological data allowed studying the effects of changing seasonal hydro-climatic variables on runoff in ways that previously had not been possible. TheseThe findings presented in this study suggest that warmer winter climates provide direct feedback on the hydrological flow regime with consequential changes to the seasonal distribution of water in the catchment linked to the inferred change in storage-water storage. This reconfiguration of flow pathways may reduce subsurface water storage capacity, with potential consequences for aquatic ecosystems, soil moisture retention, and the resilience of water supplies during dry periods.

During the winter period, large amounts of seasonally stored water in the snowpack regulate catchment water recharge and distribution to streams throughout the year [Trenberth, 2011]. In normal winters, the frozen season sustains snowpack until the spring. Our analysis demonstrated that there is a shift towards warmer winters as reflected in eight climate indices (Tmin, diurnal temperature range, AFDD <0, cold spell duration indicator, cool nights, frost days, icing days and snow days) (Fig. S5). These changes are consistent with other winter-based studies that shown more frequent and longer warm spells, and decreases in the frequency, duration, and severity of cold spells, based on both observations. In boreal catchments, snowpack

Formatted: Font colour: Auto

Formatted: Font colour: Auto

Formatted: Font colour: Auto

Formatted: Font colour: Auto

Formatted: Font colour: Auto

Formatted: Font colour: Auto

Formatted: Font colour: Auto

Formatted: Font colour: Auto

Formatted: Font colour: Auto

Formatted: Font colour: Auto

Formatted: Font colour: Auto

Formatted: Font colour: Auto

Formatted: Font colour: Auto

Formatted: Font colour: Auto

Formatted: Font colour: Auto

460 typically acts as a natural reservoir, accumulating water through the winter and gradually releasing it during the spring melt (Trenberth 2011). Under historically colder conditions, this process ensured a slow recharge of both surface and subsurface waters. However, our results show a shift towards warmer winter conditions, as evidenced by six temperature and snow-related climate indices (Table 1, Fig. S6). This warming corresponds to a significant reduction in the number of snow days and increased frequency of mid-winter thaw periods, consistent with regional and global studies (Sillmann et al. 2013, Easterling et al., 2016) and model projections (Sillmann et al., 2013). In addition to changes in temperatures, we also found a significant reduction in the number of snow days during the winter. The isotope analysis of $\delta^{18}\text{O}$ was then used to verify whether the increases in winter base flow were caused by direct winter precipitation using the SOI. The results showed that over time (from 2002 to 2022), SOI values decreased (trending from 0.2 in 2002 to -0.6 in 2022 on average), showing a shift towards winter precipitation signal confirming an increased contribution from winter precipitation to stream flow (Fig. 6B). Together, these results all suggest that the warmer winter trajectory could further enhance mid-winter melt events, rather than being stored in place as snowpack until spring melt, which leads to higher flows in streams during the frozen season.

Formatted: Font colour: Auto

475 Modelling the baseflow runoff during the winter. Isotopic analysis of $\delta^{18}\text{O}$ further confirmed that the increased winter Q_{min} is not primarily driven by higher total winter precipitation but rather by enhanced mid-winter snowmelt, which rapidly delivers precipitation to streamflow instead of storing it as snow. Supporting this, three supplementary analyses found no significant relationship between autumn conditions and mid-winter runoff (Fig. S4), suggesting that the dominant control is winter temperature, not antecedent moisture conditions. The results indicate a climatic shift in hydrological partitioning, favouring rapid surface runoff over groundwater recharge and sustained summer streamflow.

- Formatted: Font colour: Auto
- Formatted: Font colour: Auto
- Formatted: Font colour: Auto
- Formatted: Font colour: Auto
- Formatted: Font colour: Auto
- Formatted: Font colour: Auto
- Formatted: Font colour: Auto
- Formatted: Font colour: Auto
- Formatted: Font colour: Auto
- Formatted: Font colour: Auto
- Formatted: Font colour: Auto
- Formatted: Font colour: Auto
- Formatted: Font colour: Auto
- Formatted: Font colour: Auto
- Formatted: Font colour: Auto
- Formatted: Font colour: Auto
- Formatted: Font colour: Auto
- Formatted: Font colour: Auto
- Formatted: Font colour: Auto
- Formatted: Font colour: Auto
- Formatted: Font colour: Auto

480 Modelling the winter Q_{min} runoff using a stepwise linear regression showed that the best predictor was the accumulated degree days below zero (AFDD<0) (Fig. 6A), which illustrated that those warm winters with lower AFDD<0 had higher winter baseflow Q_{min} compared to the years with the colder winters with more AFDD<0. These results can be explained by the reduction in the amount of precipitation falling as snow during a shortened frozen season, an increase in the frequency of mild (>0 °C) periods and/or induce earlier induced mid-winter snowmelt as suggested by (Laternser and Schneebeli, 2003), while harsher winters (Laternser and Schneebeli 2003), as compared to colder winters that produce deeper snow cover and delayed snowmelt (Bokhorst et al., 2016; Rixen et al., 2022). A similar increase in winter runoff has also been recorded in Finland (Kasvi et al., 2019; Rutgersson et al., 2022) and in southern Sweden, with earlier lake ice break-up (58 %) between 1913–2014 (Arheimer and Lindström, 2015; Hallerbäck et al., 2022). The consequences of warmer winters have already been found to reduce soil frost (Easterling, 2002; Friesen et al., 2021; Girardin et al., 2022), alter stream runoff and timing of proceeding springs succeeding spring floods (Blöschl et al., 2017; Breton et al., 2022). However, if such conditions become more frequent, future changes in the magnitude and intensity of flooding caused by rapid snowmelt due to warmer winters could increase economic uncertainties for vulnerable areas and infrastructures (Tabari 2020, Nasr et al., 2021; Tabari, 2020) should these events become more prevalent.

(<https://www.ncei.noaa.gov/access/monitoring/nao/>) to test the correlation with seasonal hydro-climatic variables from the Krycklan catchment, we found significant correlations with four winter indices (average winter temperature, Tmin, cold spells and warm spells) and four summer temperature extreme indices (average summer temperature, Tmax, summer cold spells, summer cold days) (Fig. S7). These results suggest the observed changes in winter and summer climate could related to the much larger regional NAO system, which in turn can be key to understanding the mechanism regulating winter runoff processes.

The findings of this study emphasize the substantial implications of warm winters for hydrological processes within boreal catchments. Specifically, the observed increase in winter runoff, coupled with the altered timing and magnitude of the cold season, signals significant changes in water storage and redistribution over the course of the year. Notably, the intensified mid-winter snowmelt events appear to reduce the snowpack that would otherwise contribute to spring runoff and groundwater recharge, diminishing water availability during the critical summer months when baseflow and groundwater are most critical (Jasechko et al. 2017, Klove et al. 2017, Nygren et al. 2020). A higher risk of hydrological droughts could occur where deficits in both surface and subsurface water coincide resulting in stronger impacts on biophysical conditions and biogeochemical processes (Monson et al., 2005) (Blahušiaková et al. 2020, Teutschbein et al. 2022, Bouchard et al. 2024), water table depth, and hence aquatic organisms (Dao(Williams et al., 2024; Dubois, 2015, Kreyling et al., 2022; Nygren et al., 2021), 2019), ecological processes (Hryciuk et al., 2021), and tree growth decline (Laudon et al. 2024). While higher winter baseflow moderates spring peaks and the risk of flooding, While the isotopic analysis confirmed shifts in the relative contributions of winter precipitation to streamflow, it also highlighted the complexity of these processes. The increased winter runoff does not directly correlate with increased winter precipitation, suggesting that warmer winter temperatures and mid-winter snowmelt are the primary drivers of these changes. These results point to the potential for more frequent and severe hydrological extremes, such as flooding from rapid snowmelt combined with rain on snow in winter and water scarcity in summer, as winter warming intensifies. During the low flow regime, the strong control of stream temperature affects life in aquatic ecosystems as well as the water availability for drinking and irrigation purposes, exacerbating low reservoir levels and decreasing hydropower generation (Dierauer et al. 2018). Other implications of warmer winters and summer processes have already been shown to affect net ecosystem exchange (NEE) (Blöschl et al., 2017; Irannezhad et al., 2022)(Monson et al. 2005), the lower recharge to groundwater can result in drier summer landscapes with indirect consequences such as increased wildfire activity (Westerling et al., 2006), higher rates of tree mortality (Sterck et al., 2024), increased water stress on mountain ecosystems (Hatchett and McEvoy, 2018) and decreased uptake of carbon, water table depth (Nygren et al. 2021, Dubois et al. 2022, Dao et al. 2024), ecological processes (Hryciuk et al. 2021), and tree growth decline (Laudon et al. 2024). While higher winter runoff moderates snowmelt-related flooding (van der Woude(Blöschl et al., 2023), 2017, Irannezhad et al. 2022). Ultimately, the implications of warmer winters on proceeding seasonal runoff can be severe and warrant additional efforts in preparing for future climate changes.

, lower groundwater recharge can result in drier summer landscapes with severe consequences on wildfire activity (Westerling et al. 2006), tree mortality (Sterck et al. 2024), ecosystem stress (Hatchett and McEvoy 2018) and carbon uptake (van der

Formatted: Font colour: Auto

Formatted: Font colour: Auto

Formatted: Font colour: Auto

Formatted: Font colour: Auto

Woude et al. 2023). These implications underscore the urgent need for further research on how changes in seasonal runoff dynamics, driven by broader climatic factors like the NAO, will impact regional water resources and ecosystem functions in the future.

Conclusion

Our long-term dataset showed that dominant hydrometeorological characteristics of the boreal Krycklan catchment are changing with consequences for the catchment hydrology. Enhanced extreme In this study, we found significant trends in many warming-related climate extreme indices over the last four decades during summer and both winter suggest warming in both seasons. Warmer and summer. The warming observed in the last 40 years corroborates with the longer 130-year time series that dates to the 1890s showing progressive warming temperatures will result in shrinking snowpacks that melt earlier in the year causing the effective storage capacity of winter snowpacks to decrease. We show that warmer winters already have, and will continue to result in across time. Evaluating how these changes affect key hydrological processes during the same period, we observed higher runoff during the winter while decreasing runoff during the following summers. Using the significant trends in the extreme indices to evaluate the effects on catchment seasonal runoff, we found that winter variables were best at explaining winter minimum runoff while winter and summer maximum temperatures could explain the changes observed in summer minimum runoff. These findings were supported by water isotopic analysis that showed an increasing seasonal origin index during the winter indicating higher contributions of winter precipitation to winter runoff and consequently lower winter precipitation to summer runoff. With the decreased catchment water storage due to increased winter runoff before the occurrence of the true spring freshet, which exhausts flood, the potential for maintaining summer base flow. These findings have been supported by trends in isotopic composition suggesting changes towards winter precipitation dominating winter stream flow while summer precipitation signals dominate summer flows. baseflow runs the risk of being exhausted in the future, should warming trends persist. This research work highlights the importance of understanding future hydro-climatic changes trends where changes in the seasonal distribution of water could magnify floods or further affect low-flow conditions, as well as other with implications for drought-related issues in light of considering future climate change.

Code Availability and Data Availability

Runoff data, meteorological data and isotopes isotope data for Svartberget can be download downloaded from the SITES data portal (<https://data.fieldsites.se/portal/>). Long-term data from the Stensele station can be obtained from SMHI achieves. Codes used in the production of graphs and their associated files can be found on fig.share.com <https://doi.org/10.6084/m9.figshare.27320538>

Formatted: Font colour: Auto

Formatted: Font colour: Auto

Formatted: Font colour: Auto

Formatted: Font colour: Auto

Formatted: Font colour: Auto

Formatted: Font colour: Auto

Formatted: Font colour: Auto

Formatted: Font colour: Auto

Formatted: Font colour: Auto

Formatted: Font colour: Auto

Formatted: Font colour: Auto

Formatted: Font colour: Auto

Formatted: Font colour: Auto

Formatted: Font colour: Auto

Formatted: Font colour: Auto

Formatted: Font colour: Auto

Formatted: Font colour: Auto

Formatted: Font colour: Auto

Formatted: Font colour: Auto

Formatted: Font colour: Auto

Formatted: Font colour: Auto

Formatted: Font colour: Auto

Formatted: Font colour: Auto

Formatted: Font colour: Auto

Formatted: Font colour: Auto

Formatted: Font colour: Auto

Formatted: Font colour: Auto

Formatted: Font colour: Auto

Author contribution

HL developed the initial concept, assisted in the analysis of results, and ~~discussion~~ created the first draft of the manuscript. TT processed the data, analysed the results and wrote the first draft of the manuscript.

Competing interest

The contact author has declared that none of the authors has any competing interests.

Special issue statement

This article is part of the special issue “Northern hydrology in transition – impacts of a changing cryosphere on water resources, ecosystems, and humans (TC/HESS inter-journal SI)”. ~~It is not associated with a conference.~~

Acknowledgement

We would like to thank the staff from the SLU Unit for Field-based Forest Research for technical and logistic support.

Financial support

The study was funded by the Knut and Alice Wallenberg Foundation (grants 2018.0259; 2023.0245). The study site Svartberget is part of the Swedish Infrastructure for Ecosystem Science (SITES) and the Swedish Integrated Carbon Observation System (ICOS-Sweden) research infrastructure. Financial support from the Swedish Research Council and contributing research institutes to both SITES and ICOS-Sweden are acknowledged.

Reference

Alexander, L. V., et al. (X. Zhang, T. C. Peterson, J. Caesar, B. Gleason, A. M. G. K. Tank, M. Haylock, D. Collins, B. Trewin, F. Rahimzadeh, A. Tagipour, K. R. Kumar, J. Revadekar, G. Griffiths, L. Vincent, D. B. Stephenson, J. Burn, E. Aguilar, M. Brunet, M. Taylor, M. New, P. Zhai, M. Rusticucci, and J. L. Vazquez-Aguirre. 2006). Global observed changes in daily climate extremes of temperature and precipitation. *J Geophys Res Atmos*, 111(D5), doi:10.1029/2005jd006290.

Ali, S., A. Basit, M. Umair, and J. Ni (2024). Impacts of climate and land coverage changes on potential evapotranspiration and its sensitivity on drought phenomena over South Asia. *International Journal of Climatology*, 44(3), 812–830, doi:10.83010.1002/joc.8357.

Allen, J. von Freyberg, M. Weiler, G. R. Goldsmith, and J. W. Kirchner (2019). The Seasonal Origins of Streamwater in Switzerland. *Geophysical Research Letters*, 46(17–18), 10425–10434, doi:10.1043410.1029/2019gl084552.

Allen, and S. C. Sheridan (2015). Evaluating changes in season length, onset, and end dates across the United States (1948–2012). *International Journal of Climatology*, 36(3), 1268–1277, doi:10.127710.1002/joc.4422.

Arheimer, B., and G. Lindström (2015). Climate impact on floods: changes in high flows in Sweden in the past and the future (1911–2100). *Hydrology and Earth System Sciences*, 19(2), 771–784, doi:10.78410.5194/hess-19-771-2015.

Formatted: Font colour: Auto

Formatted: Font colour: Auto

Formatted: Font colour: Auto

Formatted: Font colour: Auto

Formatted: English (United States)

Formatted: Indent: Left: 0 cm, Hanging: 1.27 cm

Formatted: Font: Not Italic

Formatted: Font: Bold, Not Italic

Formatted: Font: Not Italic

Formatted: Font: Bold, Not Italic

Formatted: Font: Not Italic

Formatted: Font: Bold, Not Italic

Formatted: Font: Not Italic

Formatted: Font: Bold, Not Italic

Barnett, T. P., J. C. Adam, and D. P. Lettenmaier. 2005. Potential impacts of a warming climate on water availability in snow-dominated regions. *Nature*, **438**(7066), 303-309, doi:10.1038/nature04141.

Beaulieu, M., H. Schreier, and G. Jost. 2012. A shifting hydrological regime: a field investigation of snowmelt runoff processes and their connection to summer base flow, Sunshine Coast, British Columbia. *Hydrological Processes*, **26**(17), 2672-2682, doi:10.1002/hyp.9404.

Blahušáková, A., M. Matoušková, M. Jeníček, O. Ledvinka, Z. Kliment, J. Podolinská, and Z. Snopková. 2020. Snow and climate trends and their impact on seasonal runoff and hydrological drought types in selected mountain catchments in Central Europe. *Hydrological Sciences Journal*, **65**(12), 2083-2096, doi:10.1080/02626667.2020.1784900.

Blöschl, G., et al. (2016) Parajka, R. A. P. Perdigao, B. Merz, B. Arheimer, G. T. Aronica, A. Bilibashi, O. Bonacci, M. Borga, I. Canjevac, A. Castellarin, G. B. Chirico, P. Claps, K. Fiala, N. Frolova, L. Gorbachova, A. Güll, J. Hannaford, S. Harrigan, M. Kireeva, A. Kiss, T. R. Kjeldsen, S. Kohnová, J. J. Koskela, O. Ledvinka, N. Macdonald, M. Mavrova-Guirguinova, L. Mediero, R. Merz, P. Molnar, A. Montanari, C. Murphy, M. Osuch, V. Ovccharuk, I. Radevski, M. Rogger, J. L. Salinas, E. Sauquet, M. Sraj, J. Szolgay, A. Viglione, E. Volpi, D. Wilson, K. Zaimi, and N. Zivkovic. 2017. Changing climate shifts timing of European floods. *Science*, **357**(6351), 588-590, doi:10.1126/science.aan2506.

Bokhorst, S., et al. (2016) Bokhorst, S., S. H. Pedersen, L. Brucker, O. Anisimov, J. W. Bjerke, R. D. Brown, D. Ehrich, R. L. H. Essery, A. Heilig, S. Ingvald, C. Johansson, M. Johansson, I. S. Jónsdóttir, N. Inga, K. Luoju, G. Macelloni, H. Mariash, D. McLennan, G. N. Rosqvist, A. Sato, H. Savelle, M. Schneebeli, A. Sokolov, S. A. Sokratov, S. Terzaghi, D. Vikhamar-Schuler, S. Williamson, Y. B. Qiu, and T. V. Callaghan. 2016. Changing Arctic snow cover: A review of recent developments and assessment of future needs for observations, modelling, and impacts. *Ambio*, **45**(5), 516-537, doi:10.1007/s13280-016-0770-0.

Bouchard, B., D. F. Nadeau, F. Domine, F. Anttil, T. Jonas, and E. Tremblay. 2024. How does a warm and low-snow winter impact the snow cover dynamics in a humid and discontinuous boreal forest? Insights from observations and modeling in eastern Canada. *Hydrology and Earth System Sciences*, **28**(12), 2745-2765, doi:10.5194/hess-28-2745-2024.

Boumaiza, L., R. Chesnaux, J. Walter, and C. Stumpp. 2020. Assessing groundwater recharge and transpiration in a humid northern region dominated by snowmelt using vadose-zone depth profiles. *Hydrogeology Journal*, **28**(7), 2315-2329, doi:10.1007/s10040-020-02204-z.

Breton, F., M. Vrac, P. Yiou, P. Vaittinada Ayar, and A. Jézéquel. 2022. Seasonal circulation regimes in the North Atlantic: Towards a new seasonality. *International Journal of Climatology*, **42**(11), 5848-5870, doi:10.1002/joc.7565.

Cassou, C., and J. Cattiaux. 2016. Disruption of the European climate seasonal clock in a warming world. *Nature Climate Change*, **6**(6), 589-594, doi:10.1038/nclimate2969.

Chi, J. S., M. B. Nilsson, H. Laudon, A. Lindroth, J. Wallerman, J. E. S. Fransson, N. Kljun, T. Lundmark, M. O. Löfvenius, and M. Peichl. 2020. The Net Landscape Carbon Balance-Integrating terrestrial and aquatic carbon fluxes in a managed boreal forest landscape in Sweden. *Global Change Biology*, **26**(4), 2353-2367, doi:10.1111/gcb.14983.

Cleland, E. E., I. Chuine, A. Menzel, H. A. Mooney, and M. D. Schwartz. 2007. Shifting plant phenology in response to global change. *Trends Ecol. Evol. in Ecology & Evolution*, **22**(7), 357-365, doi:10.1016/j.tree.2007.04.003.

Cohen, J., et al. (J. A. Screen, J. C. Furtado, M. Barlow, D. Whittleston, D. Coumou, J. Francis, K. Dethloff, D. Entekhabi, J. Overland, and J. Jones. 2014). Recent Arctic amplification and extreme mid-latitude weather. *Nature Geoscience*, **7**(9), 627-637, doi:10.1038/ngeo2234.

Contosta, A. R., N. J. Casson, S. J. Nelson, and S. Garlick. 2020. Defining frigid winter illuminates its loss across seasonally snow-covered areas of eastern North America. *Environmental Research Letters*, **15**(3), doi:10.1510.1088/1748-9326/ab54f3.

Coplen, T. B. (1995). New Iupac Guidelines for the Reporting of Stable Hydrogen, Carbon, and Oxygen Isotope-Ratio Data. *J. Res. Natl. Inst. Stan. Journal of Research of the National Institute of Standards and Technology*, **100**(3), 285-285, doi:10.28510.6028/jres.100.021.

Formatted: Font: Not Italic

Formatted: Font: Bold, Not Italic

Formatted: Font: Not Italic

Formatted: Font: Bold, Not Italic

Formatted: Font: Not Italic

Formatted: Font: Bold, Not Italic

Formatted: Font: Not Italic

Formatted: Font: Bold, Not Italic

Formatted: Font: Not Italic

Formatted: Font: Bold, Not Italic

Formatted: Font: Not Italic

Formatted: Font: Bold, Not Italic

Formatted: Font: Not Italic

Formatted: Font: Bold, Not Italic

Formatted: Font: Not Italic

Formatted: Font: Bold, Not Italic

Formatted: Font: Not Italic

Formatted: Font: Bold, Not Italic

Formatted: Font: Not Italic

Formatted: Font: Bold, Not Italic

Formatted: Font: Not Italic

Formatted: Font: Bold, Not Italic

Formatted: Font: Not Italic

Formatted: Font: Bold, Not Italic

Formatted: Font: Not Italic

Formatted: Font: Bold, Not Italic

675 Dao, P. U., A. G. Heuzard, T. X. H. Le, J. Zhao, R. Yin, C. Shang, and C. H. Fan (2024). The impacts of climate change on groundwater quality: A review. *Sci. Science of the Total Environ.*, **912**, doi:10.1016/j.scitotenv.2023.169241.

Dierauer, J. R., P. H. Whitfield, and D. M. Allen (2018). Climate Controls on Runoff and Low Flows in Mountain Catchments of Western North America. *Water Resources Research*, **54**(10), 7495-7510, doi:10.1029/2018wr023087.

Donat, M. G., J. Sillmann, and E. M. Fischer (2020). Changes in climate extremes in observations and climate model simulations. From the past to the future. *Climate Extremes and Their Implications for Impact and Risk Assessment*, 31-57, doi:10.1016/B978-0-12-814895-2.00003-3.

680 Druckenmiller, M. L., T. Moon, and R. Thoman (2021). The Arctic. *B Am Meteorol Soc., Bulletin of the American Meteorological Society*, **102**(8), S263-S315, doi:10.1175/Bams-D-21-0086.1.

Dubois, E., M. Larocque, S. Gagné, and M. Braun (2022). Climate Change Impacts on Groundwater Recharge in Cold and Humid Climates: Controlling Processes and Thresholds. *Climate*, **10**(1), doi:10.1010.3390/cli10010006.

685 Earman, S., A. R. Campbell, F. M. Phillips, and B. D. Newman (2006). Isotopic exchange between snow and atmospheric water vapor: Estimation of the snowmelt component of groundwater recharge in the southwestern United States. *J Geophys Res Atmos*, **111**(D9), doi:10.1029/2005jd006470.

Easterling, D. R. (2002). Recent changes in frost days and the frost-free season in the United States. *B Am Meteorol Soc., Bulletin of the American Meteorological Society*, **83**(9), 1327-1332, doi:10.1175/1520-0477-83.9.1327.

Easterling, D. R., K. E. Kunkel, M. E. Wehner, and L. Q. Sun (2016). Detection and attribution of climate extremes in the observed record. *Weather Clim Extreme and Climate Extremes*, **11**, 17-27, doi:10.1016/j.wace.2016.01.001.

690 Friesen, H. C., R. A. Slesak, D. L. Karwan, and R. K. Kolka (2021). Effects of snow and climate on soil temperature and frost development in forested peatlands in minnesota, USA. *Geoderma*, **394**, doi:10.1016/j.geoderma.2021.115015.

Fu, W. X., L. Tian, Y. Tao, M. Y. Li, and H. D. Guo (2023). Spatiotemporal changes in the boreal forest in Siberia over the period 1985-2015 against the background of climate change. *Earth System Dynamics*, **14**(1), 223-239, doi:10.5194/esd-14-223-2023.

695 Girardin, M. P., J. Guo, D. Gervais, J. Metsaranta, E. M. Campbell, A. Arsenault, M. Isaac-Renton, and E. H. Hogg (2022). Cold-season freeze frequency is a pervasive driver of subcontinental forest growth. *P Natl Acad Sci USA*, **119**(18), doi:10.1073/pnas.2117464119.

700 Hallerbäck, S., L. S. Huning, C. Love, M. Persson, K. Stensen, D. Gustafsson, and A. AghaKouchak (2022). Climate warming shortens ice durations and alters freeze and break-up patterns in Swedish water bodies. *The Cryosphere*, **16**(6), 2493-2503, doi:10.5194/tc-16-2493-2022.

Hatchett, B. J., and D. J. McEvoy (2018). Exploring the Origins of Snow Drought in the Northern Sierra Nevada, California. *Earth Interact*, **22**, doi:10.1175/Ei-D-17-0027.1.

705 Hekmatzadeh, A. A., S. Kaboli, and A. Torabi Haghighi (2020). New indices for assessing changes in seasons and in timing characteristics of air temperature. *Theoretical and Applied Climatology*, **140**(3-4), 1247-1261, doi:10.1007/s00704-020-03156-w.

Hryciuk, A. R., et al. (2021). Hryciuk, A. R., P. D. F. Isles, R. Adrian, M. Albright, L. C. Bacon, S. A. Berger, R. Bhattacharya, H. P. Grossart, J. Hejzlar, A. L. Hetherington, L. B. Knoll, A. Laas, C. P. McDonald, K. Merrell, J. C. Nejtgaard, K. Nelson, P. Noges, A. M. Paterson, R. M. Pilla, D. M. Robertson, L. G. Rudstam, J. A. Rusak, S. Sadro, E. A. Silow, J. D. Stockwell, H. Yao, K. Yokota, and D. C. Pierson. 2021. Earlier winter/spring runoff and snowmelt during warmer winters lead to lower summer chlorophyll-a in north temperate lakes. *Glob Chang Biol*, **27**(19), 4615-4629, doi:10.1111/gcb.15797.

710 Hryciuk, A. R., P. D. F. Isles, D. C. Pierson, and J. D. Stockwell (2024). Winter/Spring Runoff Is Earlier, More Protracted, and Increasing in Volume in the Laurentian Great Lakes Basin. *Water Resources Research*, **60**(3), doi:10.1029/2023wr035773.

715 Huschke, R. E. (1959). *Glossary of meteorology*. American Meteorological Society, Boston.

Formatted: Font: Not Italic

Formatted: Font: Not Italic

Formatted: Font: Bold, Not Italic

Formatted: Font: Not Italic

Formatted: Font: Bold, Not Italic

Formatted: Font: Not Italic

Formatted: Font: Bold, Not Italic

Formatted: Font: Not Italic

Formatted: Font: Bold, Not Italic

Formatted: Font: Not Italic

Formatted: Font: Not Italic

Formatted: Font: Bold, Not Italic

Formatted: Font: Not Italic

Formatted: Font: Bold, Not Italic

Formatted: Font: Not Italic

Formatted: Font: Not Italic

Formatted: Font: Bold, Not Italic

Formatted: Font: Not Italic

Formatted: Font: Bold, Not Italic

Formatted: Font: Not Italic

Formatted: Font: Not Italic

720 Irannezhad, M., S. Ahmadian, A. Sadeqi, M. Minaei, B. Ahmadi, and H. Marttila. 2022. Peak Spring Flood Discharge Magnitude and Timing in Natural Rivers across Northern Finland: Long-Term Variability, Trends, and Links to Climate Teleconnections. *Water*, 14(8), doi:10.3390/w14081312.

725 Jasechko, S., L. I. Wassenaar, and B. Mayer. 2017. Isotopic evidence for widespread cold-season-biased groundwater recharge and young streamflow across central Canada. *Hydrological Processes* 31:2196-220910.1002/hyp.11175.

Jenicek, M., J. Seibert, M. Zappa, M. Staudinger, and T. Jonas. 2016. Importance of maximum snow accumulation for summer low flows in humid catchments. *Hydrology and Earth System Sciences*, 20(2), 859-874, doi:1087410.5194/hess-20-859-2016.

Karimi, S., J. Seibert, and H. Laudon. 2022. Evaluating the effects of alternative model structures on dynamic storage simulation in heterogeneous boreal catchments. *Hydrol. Res., Hydrology Research* 53(4), 562-583, doi:1058310.2166/nh.2022.121.

730 Karlsen, R. H., T. Grabs, K. Bishop, I. Buffam, H. Laudon, and J. Seibert. 2016. Landscape controls on spatiotemporal discharge variability in a boreal catchment. *Water Resources Research* 52:6541-655610.1002/2016wr019186.

Kasvi, E., E. Lotsari, M. Kumpumäki, T. Dubrovin, and N. Veijalainen. 2019. Effects of Climate Change and Flow Regulation on the Flow Characteristics of a Low-Relief River within Southern Boreal Climate Area. *Water*, 11(9), doi:10.1110.3390/w11091827.

735 Kejna, M., and A. Pospieszynska. (2023). Variability in the occurrence of thermal seasons in Poland in 1961–2020, *Meteorological Applications*, 30(4), doi:10.1002/met.2132.

Kim, Y., J. S. Kimball, K. Zhang, and K. C. McDonald. 2012. Satellite detection of increasing Northern Hemisphere non-frozen seasons from 1979 to 2008: Implications for regional vegetation growth. *Remote Sensing of Environment*, 121, 472-487, doi:1048710.1016/j.rse.2012.02.014.

740 Kinnard, C., G. Bzeouich, and A. Assani. 2022. Impacts of summer and winter conditions on summer river low flows in low elevation, snow-affected catchments. *Journal of Hydrology*, 605, doi:10.60510.1016/j.jhydrol.2021.127393.

Klove, B., H. M. L. Kvitsand, T. Pitkanen, M. J. Gunnarsdottir, S. Gaut, S. M. Gardarsson, P. M. Rossi, and I. Miettinen. 2017. Overview of groundwater sources and water-supply systems, and associated microbial pollution, in Finland, Norway and Iceland. *Hydrogeology Journal* 25:1033-104410.1007/s10040-017-1552-x.

745 Kreyling, J., et al. (K. Grant, V. Hammerl, M. A. S. Arfin-Khan, A. V. Malyshev, J. Peñuelas, K. Pritsch, J. Sardans, M. Schloter, J. Schuerings, A. Jentsch, and C. Beierkuhnlein. 2019). Winter warming is ecologically more relevant than summer warming in a cool-temperate grassland. *Sci Rep-UK*, 9, doi:10. Scientific Reports 910.1038/s41598-019-51221-w.

750 Laternser, M., and M. Schneebeli. 2003. Long-term snow climate trends of the Swiss Alps (1931-99). *International Journal of Climatology*, 23(7), 733-750, doi:1075010.1002/joc.912.

Laudon, H., et al. (2024). Laudon, H., E. M. Hasselquist, M. Peichl, K. Lindgren, R. Sponseller, F. Lidman, L. Kuglerová, N. J. Hasselquist, K. Bishop, M. B. Nilsson, and A. M. Ågren. 2021. Northern landscapes in transition: Evidence, approach and ways forward using the Krycklan Catchment Study. *Hydrological Processes*, 35(4), doi:10.3510.1002/hyp.14170.

755 Laudon, H., A. A. Mensah, J. Fridman, T. Nasholm, and S. Jamtgard. 2024. Swedish forest growth decline: A consequence of climate warming? *Forest Ecology and Management* 56510.1016/j.foreco.2024.122052.

Laudon, H., J. Seibert, S. Köhler, and K. Bishop. 2004. Hydrological flow paths during snowmelt: Congruence between hydrometric measurements and oxygen 18 in meltwater, soil water, and runoff. *Water Resources Research*, 40(3), doi:10.4010.1029/2003wr002455.

760 Laudon, H., and R. A. Sponseller. 2018. How landscape organization and scale shape catchment hydrology and biogeochemistry: insights from a long-term catchment study. *Wires Water*, 5(2), doi:10. Wiley Interdisciplinary Reviews-Water 510.1002/wat2.1265.

Laudon, H., D. Tetzlaff, C. Soulsby, S. Carey, J. Seibert, J. Buttle, J. Shanley, J. J. McDonnell, and K. McGuire. 2013. Change in winter climate will affect dissolved organic carbon and water fluxes in mid-to-high latitude catchments. *Hydrological Processes*, 27(5), 700-709, doi:1070910.1002/hyp.9686.

765 Moberg, A., et al. (2006). Moberg, A., P. D. Jones, D. Lister, A. Walther, M. Brunet, J. Jacobeit, L. V. Alexander, P. M. Della-Marta, J. Luterbacher, P. Yiou, D. Chen, A. M. G. Klein Tank, O. Saladié, J. Sigró, E. Aguilar, H. Alexandersson, C. Almarza, I. Auer, M. Barriendos, M. Begert, H. Bergström, R. Böhm, C. J. Butler, J. Caesar, A.

Formatted: Font: Not Italic

Formatted: Indent: Left: 0 cm, Hanging: 1.27 cm

Formatted: Font: Not Italic

Formatted: Font: Bold, Not Italic

Formatted: Font: Bold, Not Italic

Formatted: Indent: Left: 0 cm, Hanging: 1.27 cm

Formatted: Font: Not Italic

Formatted: Indent: Left: 0 cm, Hanging: 1.27 cm

Formatted: Font: Not Italic

Formatted: Font: Bold, Not Italic

Formatted: Font: Not Italic

Formatted: Indent: Left: 0 cm, Hanging: 1.27 cm

Formatted: Font: Not Italic

Formatted: Font: Bold, Not Italic

Formatted: Font: Not Italic

Formatted: Indent: Left: 0 cm, Hanging: 1.27 cm

Formatted: Font: Not Italic

Formatted: Font: Not Italic

Formatted: Font: Bold, Not Italic

770 Drebs, D. Founda, F. W. Gerstengarbe, G. Micela, M. Maugeri, H. Österle, K. Pandzic, M. Petrakis, L. Srnec, R. Tolasz, H. Tuomenvirta, P. C. Werner, H. Linderholm, A. Philipp, H. Wanner, and E. Xoplaki. 2006. Indices for daily temperature and precipitation extremes in Europe analyzed for the period 1901–2000. *Journal of Geophysical Research: Atmospheres*, *111*(D22), doi:10.11110.1029/2006jd007103.

775 Monson, R. K., J. P. Sparks, T. N. Rosenstiel, L. E. Scott-Denton, T. E. Huxman, P. C. Harley, A. A. Turnipseed, S. P. Burns, B. Backlund, and J. Hu. 2005. Climatic influences on net ecosystem CO exchange during the transition from wintertime carbon source to springtime carbon sink in a high-elevation, subalpine forest. *Oecologia*, *146*(1), 130–147, doi:10.14710.1007/s00442-005-0169-2.

Murray, J., J. Ayers, and A. Brookfield. 2023. The impact of climate change on monthly baseflow trends across Canada. *Journal of Hydrology*, *618*, doi:10.61810.1016/j.jhydrol.2023.129254.

780 Nasr, A., I. Björnsson, D. Honfi, O. L. Ivanov, J. Johansson, and E. Kjellström. 2021. A review of the potential impacts of climate change on the safety and performance of bridges. *Sustain Resil Infras. Sustainable and Resilient Infrastructure*, *6*(3–4), 192–242, doi:10.1080/23789689.2019.1593003.

Nygren, M., M. Giese, and R. Barthel. 2021. Recent trends in hydroclimate and groundwater levels in a region with seasonal frost cover. *Journal of Hydrology*, *602*, doi:10.60210.1016/j.jhydrol.2021.126732.

785 Nygren, M., M. Giese, B. Kløve, E. Haaf, P. M. Rossi, and R. Barthel. 2020. Changes in seasonality of groundwater level fluctuations in a temperate-cold climate transition zone. *Journal of Hydrology X*, *8*, doi:10.810.1016/j.hydroa.2020.100062.

Park, B.-J., S.-K. Min, and E. Weller. 2021. Lengthening of summer season over the Northern Hemisphere under 1.5 °C and 2.0 °C global warming. *Environmental Research Letters*, *17*(1), doi:10.1710.1088/1748-9326/ac3f64.

790 Peng, S. S., S. L. Piao, P. Ciais, P. Friedlingstein, L. M. Zhou, and T. Wang. 2013. Change in snow phenology and its potential feedback to temperature in the Northern Hemisphere over the last three decades. *Environmental Research Letters*, *8*(1), doi:10.810.1088/1748-9326/8/1/014008.

Peralta-Tapia, A., C. Soulsby, D. Tetzlaff, R. Sponseller, K. Bishop, and H. Laudon. 2016. Hydroclimatic influences on non-stationary transit time distributions in a boreal headwater catchment. *Journal of Hydrology*, *543*, 7–16, doi:10.1016/j.jhydrol.2016.01.079.

795 Rantanen, M., A. Y. Karpechko, A. Lipponen, K. Nordling, O. Hyvärinen, K. Ruosteenoja, T. Vihma, and A. Laaksonen. 2022. The Arctic has warmed nearly four times faster than the globe since 1979. *Commun. Earth Environ.*, *3*(1), doi:10.1038/s43247-022-00498-3.

Reeves, J., J. Chen, X. L. L. Wang, R. Lund, and Q. Q. Lu. 2007. A review and comparison of changepoint detection techniques for climate data. *J Appl Meteorol Clim.*, *Journal of Applied Meteorology and Climatology*, *46*(6), 900–915, doi:10.1175/Jam2493.1.

800 Rixen, C., et al. (2022). Winters are changing: snow effects on Arctic and alpine tundra ecosystems. *Arct Sci*, *8*(3), 572–608, doi:10.1139/as-2020-0058.

Ruosteenoja, K., J. Räisänen, A. Venäläinen, and M. Kämäräinen (2015). Projections for the duration and degree days of the thermal growing season in Europe derived from CMIP5 model output. *International Journal of Climatology*, *36*(8), 3039–3055, doi:10.1002/joc.4535.

805 Rixen, C., T. T. Hoyer, P. Macek, R. Aerts, J. M. Alatalo, J. T. Anderson, P. A. Arnold, I. C. Barrio, J. W. Bjerke, M. P. Björkman, D. Blok, G. Blume-Werry, J. Boike, S. Bokhorst, M. Carbognani, C. T. Christiansen, P. Convey, E. J. Cooper, J. H. C. Cornelissen, S. J. Coulson, E. Dorrepaal, B. Elberling, S. C. Elmendorf, C. Elphinstone, T. G. W. Forte, E. R. Frei, S. R. Geange, F. Gehrmann, C. Gibson, P. Grogan, A. H. Halbritter, J. Harte, G. H. R. Henry, D. W. Inouye, R. E. Irwin, G. Jespersen, I. S. Jónsdóttir, J. Y. Jung, D. H. Klimes, G. Kudo, J. Lämsä, H. Lee, J. J. Lembrechts, S. Lett, J. S. Lynn, H. M. R. Mann, M. Mastepanov, J. Morse, I. H. Myers-Smith, J. Olofsson, R. Paavola, A. Petraglia, G. K. Phoenix, P. Semenchuk, M. B. Siewert, R. Slatyer, M. J. Spasojevic, K. Suding, P. Sullivan, K. L. Thompson, M. Väisänen, V. Vandvik, S. Venn, J. Walz, R. Way, J. M. Welker, S. Wipf, and S. W. Zong. 2022. Winters are changing: snow effects on Arctic and alpine tundra ecosystems. *Arctic Science*, *8*:572–608. doi:10.1139/as-2020-0058.

815 Rutgeresson, A., et al. (E. Kjellström, J. Haapala, M. Stendel, I. Danilovich, M. Drews, K. Jylhä, P. Kujala, X. G. Larsén, K. Halsnæs, I. Lehtonen, A. Luomaranta, E. Nilsson, T. Olsson, J. Särkkä, L. Tuomi, and N. Wasmund. 2022).

Formatted: Font: Not Italic

Formatted: Font: Not Italic

Formatted: Font: Bold, Not Italic

Formatted: Font: Not Italic

Formatted: Font: Bold, Not Italic

Formatted: Font: Not Italic

Formatted: Font: Not Italic

Formatted: Font: Not Italic

Formatted: Font: Not Italic

Formatted: Font: Not Italic

Formatted: Font: Bold, Not Italic

Formatted: Font: Not Italic

Formatted: Font: Bold, Not Italic

Formatted: Indent: Left: 0 cm, Hanging: 1.27 cm

Natural hazards and extreme events in the Baltic Sea region. *Earth System Dynamics*, **13**(1), 251–304, doi:10.5194/esd-13-251-2022.

820 Schenk, F., M. Välranta, F. Muschitiello, L. Tarasov, M. Heikkilä, S. Björck, J. Brandefelt, A. V. Johansson, J. O. Näslund, and B. Wohlfarth. 2018. Warm summers during the Younger Dryas cold reversal. *Nature Communications* **9**10.1038/s41467-018-04071-5.

Schwartz, M. D., and T. M. Crawford. 2001. Detecting energy balance modifications at the onset of spring. *Phys Geogr.* **22**(5), 394–409, doi:10.1080/02723646.2001.10642751.

825 Seidl, R., et al. (2020). Seidl, R., J. Honkaniemi, T. Aakala, A. Aleinikov, P. Angelstam, M. Bouchard, Y. Boulanger, P. J. Burton, L. De Grandpré, S. Gauthier, W. D. Hansen, J. U. Jepsen, K. Jogiste, D. D. Kneeshaw, T. Kuuluvainen, O. Lisitsyna, K. Makoto, A. S. Mori, D. S. Pureswaran, E. Shorohova, E. Shubnitsina, A. R. Taylor, N. Vladimirova, F. Vodde, and C. Senf. 2020. Globally consistent climate sensitivity of natural disturbances across boreal and temperate forest ecosystems. *Ecography*, **43**(7), 967–978, doi:10.1111/ecog.04995.

830 Sillmann, J., V. V. Kharin, X. Zhang, F. W. Zwiers, and D. Bronaugh. 2013. Climate extremes indices in the CMIP5 multimodel ensemble: Part 1. Model evaluation in the present climate. *J Geophys Res Atmos., Journal of Geophysical Research-Atmospheres*, **118**(4), 1716–1733, doi:10.1029/2012JD018203.

Simons, W. D. (1967). Effects of temperature on winter runoff *Rep.*, U.S. Geological Survey, WRD, Menlo Park, California, USA.

835 Sterck, F. J., Y. J. Song, and L. Poorter. 2024. Drought- and heat-induced mortality of conifer trees is explained by leaf and growth legacies. *Sci Adv.*, **10**(15), doi:10.1126/sciadv.adl4800.

Stieglitz, M., A. Ducharme, R. Koster, and M. Suarez. 2001. The impact of detailed snow physics on the simulation of snow cover and subsurface thermodynamics at continental scales. *J Hydrometeorol., Journal of Hydrometeorology* **2**(3), 228–242, doi:10.1175/1525-7541(2001)002<0228:Tiodsp>2.0.Co;2.

840 Tabari, H. (2020). Climate change impact on flood and extreme precipitation increases with water availability (vol 10, 13768, 2020). *Sci Rep - Uk.*, **10**(1), doi:10.1038/s41598-020-74038-4.

Team, R. C. (2021). R: A language and environment for statistical computing, edited, R Foundation for Statistical Computing, Vienna, Austria.

845 Teutschbein, C., B. Q. Montano, A. Todorovic, and T. Grabs. 2022. Streamflow droughts in Sweden: Spatiotemporal patterns emerging from six decades of observations. *J Hydrol Reg Stud.*, **42**, doi:10.1016/j.ejrh.2022.101171.

Tiwari, T., R. A. Sponseller, and H. Laudon. 2018. Extreme Climate Effects on Dissolved Organic Carbon Concentrations During Snowmelt. *Journal of Geophysical Research-Biogeosciences* **123**:1277–1288. doi:10.1002/2017JG004272.

850 Tiwari, T., R. A. Sponseller, and H. Laudon. 2019. Contrasting responses in dissolved organic carbon to extreme climate events from adjacent boreal landscapes in Northern Sweden. *Environmental Research Letters* **14**10.1088/1748-9326/ab23d4.

Trenberth, K. E. (1983). What Are the Seasons. *B Am Meteorol Soc., Bulletin of the American Meteorological Society* **64**(11), 1276–1282, doi:10.1175/1520-0477.

855 Trenberth, K. E. (2011). Changes in precipitation with climate change. *Clim Res., Climate Research*, **47**(1–2), 123–138, doi:10.13810/3354/cr00953.

Ulen, B., E. Lewan, K. Kyllmar, M. Blomberg, and S. Andersson. 2019. Impact of the North Atlantic Oscillation on Swedish Winter Climate and Nutrient Leaching. *Journal of Environmental Quality* **48**:941–949. doi:10.2134/jeq2018.06.0237.

860 van der Woude, A. M., et al. (W. Peters, E. Joetzier, S. Lafont, G. Koren, P. Ciais, M. Ramonet, Y. D. Xu, A. Bastos, S. Botia, S. Stch, R. de Kok, T. Kneuer, D. Kubistin, A. Jacotot, B. Loubet, P. H. Herig-Coimbra, D. Loustau, and I. T. Lujikx. 2023). Temperature extremes of 2022 reduced carbon uptake by forests in Europe. *Nature Communications*, **14**(1), doi:10.1038/s41467-023-41851-0.

Van Loon, A. F., and G. Laaha. 2015. Hydrological drought severity explained by climate and catchment characteristics. *Journal of Hydrology*, **526**, 3–14, doi:10.1016/j.jhydrol.2014.10.059.

865 Venäläinen, A., I. Lehtonen, M. Laapas, K. Ruosteenoja, O. P. Tikkanen, H. Viiri, V. P. Ikonen, and H. Peltola. 2020. Climate change induces multiple risks to boreal forests and forestry in Finland: A literature review. *Global Change Biol., Biology* **26**(8), 4178–4196, doi:10.1111/gcb.15183.

Formatted: Font: Not Italic

Formatted: Font: Bold, Not Italic

Formatted: Indent: Left: 0 cm, Hanging: 1.27 cm

Formatted: Font: Bold, Not Italic

Formatted: Font: Not Italic

Formatted: Font: Bold, Not Italic

Formatted: Font: Bold, Not Italic

Formatted: Font: Bold, Not Italic

Formatted: Indent: Left: 0 cm, Hanging: 1.27 cm

Formatted: Indent: Left: 0 cm, Hanging: 1.27 cm

Formatted: Font: Bold, Not Italic

Formatted: Font: Bold, Not Italic

Formatted: English (United States)

Formatted: Indent: Left: 0 cm, Hanging: 1.27 cm

Formatted: Font: Not Italic

Formatted: Font: Not Italic

Formatted: Font: Bold, Not Italic

Formatted: Font: Not Italic

Formatted: Font: Bold, Not Italic

Way, D. A. (2011). Tree phenology responses to warming: spring forward, fall back? *Tree Physiology*, **31**(5), 469-471, doi:10.1093/treephys/tpr044.

Westerling, A. L., H. G. Hidalgo, D. R. Cayan, and T. W. Swetnam (2006). Warming and earlier spring increase western US forest wildfire activity. *Science*, **313**(5789), 940-943, doi:10.1126/science.1128834.

White, D., et al. (L. Hinzman, L. Alessa, J. Cassano, M. Chambers, K. Falkner, J. Francis, W. J. Gutowski, M. Holland, R. M. Holmes, H. Huntington, D. Kane, A. Kliskey, C. Lee, J. McClelland, B. Peterson, T. S. Rupp, F. Straneo, M. Steele, R. Woodgate, D. Yang, K. Yoshikawa, and T. Zhang. 2007). The arctic freshwater system: Changes and impacts. *J Geophys Res Biogeo*, **112**(G4), doi:10.1029/2006jg000353.

Williams, C. M., H. A. Henry, and B. J. Sinclair (2015). Cold truths: how winter drives responses of terrestrial organisms to climate change. *Biol Rev Camb Philos Soc*, **90**(1), 214-235, doi:10.1111/brv.12105.

Wilmking, M., et al. (M. van der Maaten-Theunissen, E. van der Maaten, T. Scharnweber, A. Buras, C. Biermann, M. Gurskaya, M. Hallinger, J. Lange, R. Shetti, M. Smiljanic, and M. Trouillier. 2020). Global assessment of relationships between climate and tree growth. *Global Change Biol*, **26**(6), 3212-3220, doi:10.1111/gcb.15057.

Zschenderlein, P., A. H. Fink, S. Pfahl, and H. Wernli (2019). Processes determining heat waves across different European climates. *Q J Roy Meteor Soc*, **145**(724), 2973-2989, doi:10.1002/qj.3599.

Formatted: Font: Not Italic

Formatted: Font: Bold, Not Italic

Formatted: Font: Not Italic

Formatted: Font: Bold, Not Italic

Formatted: Font: Not Italic, Swedish (Sweden)

Formatted: Font: Bold, Not Italic, Swedish (Sweden)

Formatted: Font: Not Italic

Formatted: Font: Bold, Not Italic

Formatted: Font: Bold, Not Italic

Formatted: Font colour: Auto

Formatted: Font colour: Auto

Formatted: Left